International Immunopharmacology 124 (2023) 110990

Contents lists available at ScienceDirect

International Immunopharmacology

journal homepage: www.elsevier.com/locate/intimp

Absent in melanoma 2 (AIM2) positive profile identifies a poor prognosis of lung adenocarcinoma patients

Chiara Colarusso [a], Michela Terlizzi [a], Anna Falanga [a], Georgious Stathopoulos [b], Luigi De Lucia [a], Phillip M. Hansbro [c], Aldo Pinto [a], Rosalinda Sorrentino [a,*]

[a] Department of Pharmacy, University of Salerno, Italy
[b] Laboratory for Molecular Respiratory Carcinogenesis, Department of Physiology, Faculty of Medicine, University of Patras, Patras, Greece
[c] Centre for Inflammation, Centenary Institute and University of Technology Sydney (UTS), School of Life Sciences, Faculty of Science, Sydney, NSW 2007, Australia

ARTICLE INFO

Keywords:
Smoke
Smoking habit
Lung adenocarcinoma
AIM2 inflammasome
Transcriptomic signature

ABSTRACT

The absent in melanoma 2 (AIM2) inflammasome has been demonstrated as involved in tumor growth. In this study we used human samples of lung adenocarcinoma (LUAD) patients, taking advantage of a mouse model of smoking cessation. Human samples were stratified according to the smoking status, high-risk factor for this type of tumor. Both public transcriptomic and human samples obtained by a clinical trial proved that AIM2 was upregulated either in terms of mRNA or protein, respectively, in the tumor mass according to the TNM stage, but it did not relate to the smoking status, age and sex. The upregulation of AIM2 was correlated to an immunosuppressive environment according to resting/non-active dendritic cells (DCs) and T regulatory cells, as demonstrated in both human samples and by means of an experimental model of smoking mice. Computational analysis showed that AIM2 upregulation was correlated to both an inflammasome profile, responsible for the poor prognosis of non-smoker and smoker LUAD patients, and to a non-inflammasome profile for former smoker.

In conclusion, our study demonstrated that AIM2 is involved in lung carcinogenesis either in a canonical and non-canonical manner due to an immunosuppressive microenvironment associated to a dismal prognosis of LUAD patients.

1. Introduction

Cigarette smoke is the leading cause and high-risk factor of respiratory disorders, such as chronic obstructive pulmonary disease (COPD) and lung cancer [1]. The latter is the second most diagnosed cancer and the leading cause of cancer-related death worldwide [2,3]. People with a history of smoking are 15–30 times more susceptible to develop lung cancer than people who never smoke [4]. Specifically, cigarette smoking plays a key role in the development and progression of lung adenocarcinoma (LUAD), the major histological subtypes of non-small cell lung cancer (NSCLC). However, almost 40 % of people who stop smoking from more than 15 years (former smokers) is still at high-risk to develop LUAD. The incidence of NSCLC, specifically LUAD, in former smokers is around 10 % for subjects who stopped smoking for >15 years, and 16 % for subjects who were heavy smokers and stopped smoking for <15 years [5]. This highlights that molecular or cellular mechanism/s induced by smoking contribute to malignant transformation in the lung even after cessation. In addition, it has to be considered that never smokers (around 10–20 % of lung cancer cases) can still undergo NSCLC development, suggesting that other external or endogenous patient-dependent factors may contribute to the development of lung tumor.

To understand the molecular mechanism/s that underlie the development of LUAD in never, former and smokers, we focused our attention on an inflammasome-dependent pathway, related to the Absent in melanoma 2 (AIM2) inflammasome, that we already demonstrated to be involved in lung carcinogenesis in smoking mice and COPD-associated LUAD [6,7].

Inflammasomes are intracellular multimeric complexes and associated with the activation of caspase-1 and the ensuing release of the activated pro-inflammatory cytokines IL-1β and IL-18 [8]. Inflammasomes have been suggested to be involved in different forms of cancer, including lung cancer [9]. Alternatively, non-canonical inflammasomes engage caspase-11 (also known as caspase-4 in humans) which can induce the release of alarmins such as IL-1α, IL-1β, IL-18 and High Mobility Group 1 (HMGB1) [10]. AIM2 is widely known as a cytosolic receptor that recognizes double-stranded DNA (dsDNA), constitutively

* Corresponding author at: Department of Pharmacy (DIFARMA), University of Salerno, Via Giovanni Paolo II 132, Fisciano 84084, Salerno, Italy.
E-mail address: rsorrentino@unisa.it (R. Sorrentino).

https://doi.org/10.1016/j.intimp.2023.110990
Received 22 June 2023; Received in revised form 4 September 2023; Accepted 22 September 2023
Available online 17 October 2023

expressed in hematopoietic cells [10–12] and is composed of C-terminal HIN-200 domain and N-terminal pyrin domain. Binding of dsDNA, either derived from microbial pathogens or from host following cell damage, to the HIN-200 domain of AIM2 initiates the oligomerization of the adaptor protein ASC (apoptosis-associated speck-like protein containing a caspase recruitment domain) leading to the assembly of the inflammasome complex that triggers an inflammatory cascade [10]. In our previous studies, we demonstrated that the inflammasome and its related cytokines participate to lung tumor growth both in a mouse model of N-methyl-N-nitrosourea (NMU)-induced lung cancer and in human samples of NSCLC [13,14]. We found that human lung tumor masses were highly populated by tolerogenic plasmacytoid dendritic cells (pDCs), able to produce high levels of IL-1α, strongly correlated with the activation of AIM2 inflammasomes [15]. In support, others demonstrated that AIM2 can serve as an oncogenic inflammatory pathway correlated to growth and proliferation of NSCLC cells both *in vitro* and *in vivo* studies [16,17]. In addition, the AIM2 inflammasome plays a role in the inflammatory pattern observed in chronic pulmonary diseases such as idiopathic pulmonary fibrosis [18] and COPD [19–21], the latter is a respiratory pathology strictly correlated with cigarette smoking and lung cancer development. Thus, based on this knowledge, the main goal of this study was to understand the involvement of AIM2 during smoking-induced inflammatory pathways that underlie LUAD progression.

2. Materials and methods

2.1. Human samples

Samples were obtained from non-smoker (n = 8), smoker (n = 16) and former smoker (n = 12) patients with a diagnosis of operable LUAD. Patients underwent surgical resection with curative intent between 02/2011–09/2015 at Asklepios Medical Center. Lung adenocarcinoma patients were enrolled in the Gauting locoregional lung adenocarcinoma donors (GLAD) study [22]. This was conducted in accordance with the Helsinki Declaration, reported in accordance with STROBE, approved by the LMU Ethics Committee (#623-15), registered with the German Clinical Trials Register, and all patients gave written informed consent. For each patient gender, age, smoking habits, and tumor stage were recorded (Table 1). Matched tumor and normal lung tissue were obtained from each patient during thoracic surgery. Samples from the tumor mass were defined 'tumor tissues' whereas 'non-cancerous tissues' were obtained from the same patient from a distant section than the tumor mass and indicated as 'normal tissue'. Normal and tumor specimens were formalin-fixed and paraffin-embedded and were cut for immunostaining.

2.2. Immunohistochemistry

Human sample of lung tissues were embedded in paraffin and were cut into 5 μm-thick sections. Primary anti-AIM2 (Proteintech Group, USA) antibody was used for immunohistochemistry analyses, as previously reported [6]. The diaminobenzidine (DAB) system was used as the chromogenic substrate to detect complexes (EnVision; Dako, Glostrup, Denmark). A solution of horse radish peroxidase-conjugated ready-to-use was used as isotype control (EnVision; Dako, Glostrup, Denmark). Lung sections were photographed with an AxioLab.A1 (Zeiss) at a magnification of 40x. AIM2 positive staining (positive area expressed as μm^2) was scored by blinded observers using ImageJ software (NIH, USA).

Table 1
GLAD study patients.

Patient	Gender	Age (years)	Smoking intensity (pack/year)	Smoking abstinence (years)	Tumor stage
Non-Smoker #1	Female	69	–	–	II
Non-Smoker #2	Female	81	–	–	I
Non-Smoker #3	Female	69	–	–	IV
Non-Smoker #4	Male	74	–	–	II
Non-Smoker #5	Female	67	–	–	I
Non-Smoker #6	Male	74	–	–	III
Non-Smoker #7	Female	64	–	–	IV
Non-Smoker #8	Female	61	–	–	I
Smoker #1	Male	44	20	–	IV
Smoker #2	Female	73	20	–	II
Smoker #3	Female	64	60	–	III
Smoker #4	Male	48	40	–	I
Smoker #5	Female	47	40	–	II
Smoker #6	Female	53	20	–	IV
Smoker #7	Female	63	45	–	IV
Smoker #8	Female	65	60	–	II
Smoker #9	Female	72	40	–	I
Smoker #10	Male	68	60	–	II
Smoker #11	Male	50	60	–	I
Smoker #12	Female	40	40	–	II
Smoker #13	Female	58	40	–	I
Smoker #14	Female	52	70	–	III
Smoker #15	Male	64	60	–	III
Smoker #16	Female	69	70	–	I
Former Smoker #1	Male	68	10	25	I
Former Smoker #2	Male	79	20	11	I
Former Smoker #3	Male	69	60	2	II
Former Smoker #4	Male	74	40	2	II
Former Smoker #5	Male	72	5	11	III
Former Smoker #6	Male	81	100	11	III
Former Smoker #7	Female	58	45	1	I
Former Smoker #8	Female	69	40	2	I
Former Smoker #9	Male	58	60	6	II
Former Smoker #10	Male	64	40	11	III
Former Smoker #11	Male	77	10	10	III
Former Smoker #12	Female	59	40	0.5	I

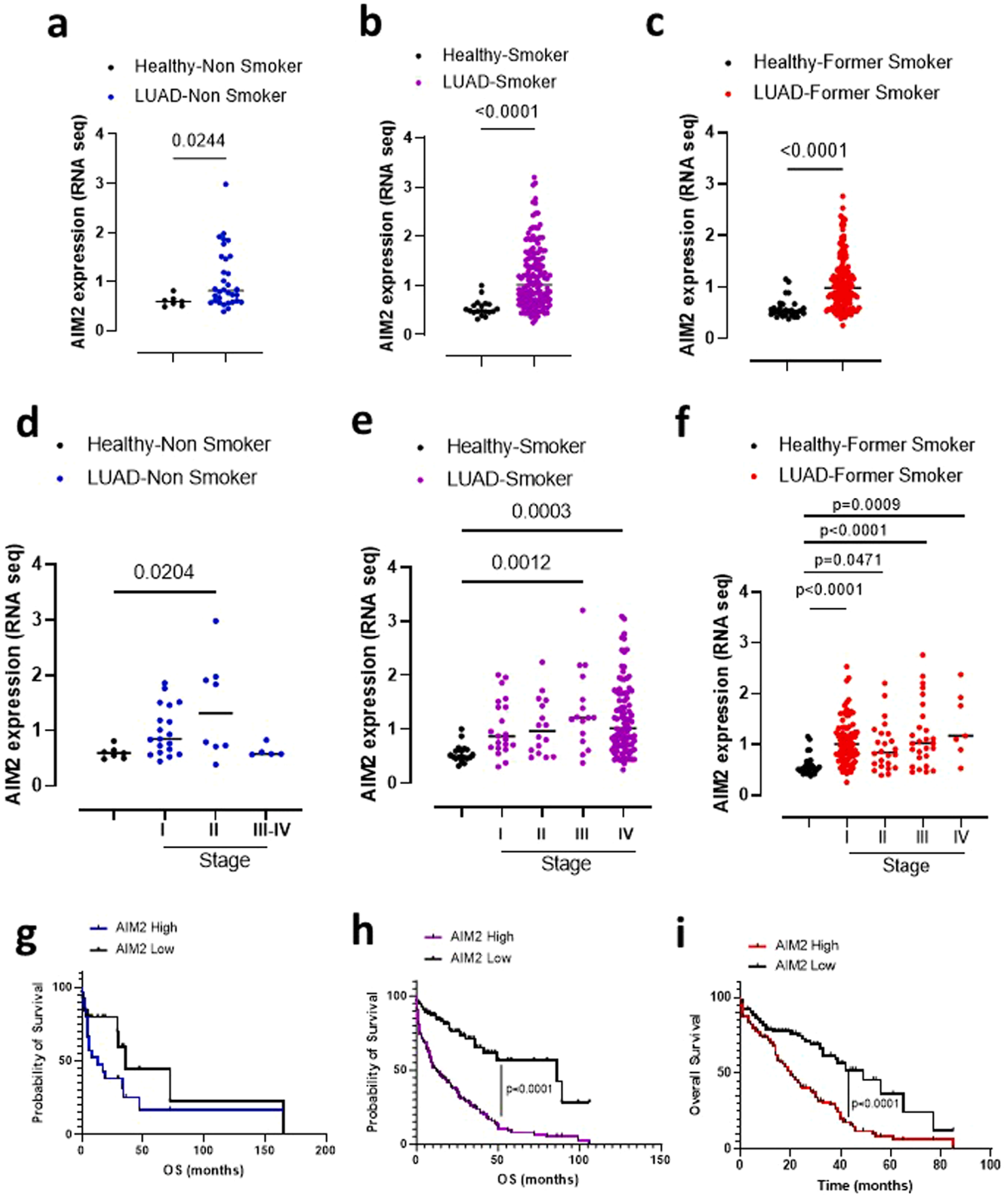

Fig. 1. Expression levels of AIM2 mRNA and survival rate of Non-Smoker, Smoker and Former Smoker LUAD patients. Scatter dot plots represent the differences in RNA levels of AIM2 in Healthy, non-cancerous, and LUAD, tumoral tissues in (**a**) Non-Smoker, (**b**) Smoker and (**c**) Former Smoker LUAD patients. AIM2 mRNA expression was evaluated according to the TNM stage in (**d**) Non-Smoker, (**1e**) Smoker and (**f**) Former Smoker LUAD patients. Survival curve of (**g**) Non-Smoker, (**h**) Smoker and (**i**) Former Smoker patients with LUAD according to AIM2 expression associated with a cut-off calculated using ROC analysis. Data in Fig. 1a–f are expressed as median and statistical analysis was performed using the Mann–Whitney *U* test. Black dots indicated Healthy, non-cancerous tissue; blue, violet and red dots indicated tumoral tissues from Non-Smoker, Smoker and Former Smoker LUAD, respectively. Log-rank test was performed to statistically analyze the survival rate between the groups. (For interpretation of the references to colour in this figure legend, the reader is referred to the web version of this article.)

2.3. Mice

Female specific pathogen-free C57BL/6N mice (6–8 weeks of age, Charles River Laboratories, Lecco, Italy) were fed a standard chow diet and maintained in specific pathogen-free conditions at the animal care facility of Department of Pharmacy, University of Salerno. All animal experiments were performed under protocols that followed the Italian (D.L. 26/2014) and European Community Council for Animal Care (2010/63/EU). This study was carried out in strict accordance with the recommendations in the Guide for Care and Use of Laboratory Animals of the Instituto Nazionale per la Salute, Italy. The experimental protocol was approved by the Committee on Ethics for Animal Studies of the

Table 2
AIM2 mRNA levels in Healthy vs Non-Smoker, Smoker and Former Smoker LUAD samples.

	Healthy-Non Smoker	LUAD-Non Smoker	Healthy-Smoker	LUAD-Smoker	Healthy-Former Smoker	LUAD-Former Smoker
Number of patients	**7**	**32**	**19**	**147**	**30**	**142**
Minimum	0.4863	0.3857	0.3169	0.2450	0.3808	0.2551
25 % Percentile	0.5025	0.5865	0.4584	0.6874	0.4669	0.6737
Median	**0.5939**	**0.8125**	**0.4882**	**1.017**	**0.5307**	**0.9782**
75 % Percentile	0.6460	1.498	0.6197	1.566	0.6141	1.317
Maximum	0.8113	2.984	1.002	3.202	1.155	2.762
Range	0.3249	2.598	0.6855	2.957	0.7741	2.507
95 % CI of median	98.44 %	97.99 %	98.08 %	95.26 %	95.72 %	96.45 %
Actual confidence level	98.44 %	97.99 %	98.08 %	95.26 %	95.72 %	96.45 %
Lower confidence limit	0.4863	0.6118	0.4584	0.8681	0.4859	0.8627
Upper confidence limit	0.81131.915	1.1881.972	0.61972.519	1.1990.5492	0.58653.088	1.0810.615
Kurtosis index						

Table 3
Data from ROC analysis.

	Non-Smoker	Smoker	Former Smoker
AUC	0.7723	0.85	0.8362
Cut-off (read counts)	0.69	0.62	0.59
Sensitivity (%)	65.63 %	78.91 %	80.3 %
Sensitivity 95 % CI	48.31 % to 79.59 %	71.62 % to 84.73 %	72.98 % to 85.99 %
Specificity (%)	85.71 %	78.95 %	77 %
Specificity 95 % CI	48.69 % to 99.27 %	56.67 % to 91.49 %	59.07 % to 88.2.1 %

Table 4
Overall survival rate.

	Non Smoker, n = 27		Smoker, n = 138		Former Smoker; n = 134	
	$AIM2^+$	$AIM2^-$	$AIM2^+$	$AIM2^-$	$AIM2^+$	$AIM2^-$
Overall survival (months)	13	36	12	86	20	49
Hazard ratio ($AIM2^+$ vs $AIM2^-$)	1.7		3.3		2.3	

University of Salerno and the Italian Health Ministry with the approval number 985/2017.

2.4. Cigarette smoke exposure protocol

To mimic the effect of smoking cessation in mice, animals were exposed to first-hand cigarette smoke for 4 weeks using a nose-only chamber (EMMS, UK) as previously described [6] followed by a 16-week cessation period (Former group). Briefly, mice were exposed for 4 weeks to first-hand cigarette smoke once a day, 5 days/week, at the concentration of 1 $\mu g/cm^3$ of total particular matter (TPM), generated from Red Marlboro cigarettes. Control mice, defined as Room Air group, breathed filtered air for the same time. Mice were sacrificed 24 h after the last CS exposure.

2.5. Sample collection

Blood samples were collected from the orbital sinus using a Pasteur pipette and sera were separated as standard and hemolyzed specimens discarded. Broncho-alveolar lavage (BAL) was collected using 0.5 mL of PBS containing 0.5 mM EDTA to measure pro- and anti-inflammatory cytokines levels. Right lung lobes were collected and digested with collagenase (1 U/mL, Sigma Aldrich, Rome, Italy) for flow cytometry analysis (FACS) analysis and to perform ELISAs analysis. Left lung lobes were embedded into OCT medium to perform hematoxylin and eosin (H&E, histology) staining, Periodic acid/Alcian blue/Schiff (PAS, inflammation) and Masson's trichrome (fibrosis) staining.

2.6. Lung histology

For histological examination, left lung lobe cryosections were cut 7 μm-thick, and stained by using H&E, PAS and Masson's trichrome stains. H&E-stained slides were used to assess air space enlargement using the mean linear intercept (MLI) technique, which is the standard method of assessing alveolar diameter and emphysema in mice [6,23,24]. Masson's trichrome stained cryosections were analyzed to assess collagen deposition and fibrotic lung areas, which were expressed as positive-stained area (μm^2) and quantified using ImageJ software. PAS stained cryosections were used to evaluate the effect of smoking cessation on lung inflammation following smoke exposure and cessation. The degree of inflammation, which correlates with the detection of glycoprotein, was scored by blinded observers. PAS + cryosections were graded with scores 0 to 4 to describe low to severe lung inflammation as follows: 0: <5%; 1: 5–25 %; 2: 25–50 %; 3: 50–75 %; 4: <75 % positive staining/total lung area [25].

2.7. Flow cytometry analysis

To investigate the composition of lung infiltrating immune cells we performed flow cytometry (BD FacsCalibur Milan, Italy) on lung homogenates. Lung cell suspensions were stained with the following antibodies: CD11b, CD11c, F4/80, MHC II, Gr-1, CD4, CD25, FoxP3 and AIM2. Cells were firstly stained for the extracellular factors CD11b, CD11c, F4/80, MHC II, Gr-1, CD4 and CD25 and then fixed and permeabilized using BD Cytofix/Cytoperm solutions before adding anti-AIM2 and anti-FoxP3.

2.8. Cytokine measurements

IL-1α, IL-33, and TGF-β were measured in lung homogenates and IL-1β, IL-18, TNF-α, IL-10 levels were measured in BAL samples. The assays were performed using commercially available ELISA kits (eBioscience, CA, USA; R&D Systems, Bio-Techne, Minneapolis, USA). Cytokine levels in lung homogenates are expressed as pg/mg protein and in BAL samples as pg/mL.

2.9. Lactate dehydrogenase (LDH) levels

Levels of LDH were measured in serum samples collected from Room Air and Former Smoker groups using a commercially available kit (Sigma, Italy) following the manufacturer's instructions. Data are expressed as LDH U/mL.

2.10. RNA-seq data analysis

Public Cancer Genome Atlas (TCGA_LUAD) repository comprising

Table 5
Multivariate analysis of AIM2 + LUAD patients considering several clinical variables.

Variable	Category	AIM2 + Non-Smoker			AIM2 + Smoker			AIM2 + Former Smoker		
		n (%)	95 % CI	P value	n (%)	95 % CI	P value	n (%)	95 % CI	P value
Stage	***I***	13 (61.9)		Reference	18 (42.9)		Reference	56 (57.1)	–	Reference
	II	7 (33.3)	0.4024 to 1.688	**0.0047**	11 (26.2)	−0.5732 to 0.3619	0.6485	18 (18.4)	−0.3766 to 0.1813	0.4883
	III	0 (0)	–	–	13 (69)	−0.1128 to 0.7751	0.1385	18 (18.4)	−0.04048 to 0.5446	0.0903
	IV	1 (4.8)	−1.711 to 0.5819	0.2982	–	–	–	6 (6.1)	−0,04330 to 0,8606	0.0758
Oncogene	***Positive***	19 (90.5)	–	Reference	20 (46.5)	–	Reference	65 (63.7)	–	Reference
	Negative	2 (9.5)	−0.8981 to 1.432	0.6205	23 (53.5)	−0.2210 to 0.5243	0.4132	37 (36.3)	−0.1988 to 0.2312	0.8813
Sex	***Female***	15 (71.4)	–	Reference	23 (54.7)	–	Reference	65 (63.7)	–	Reference
	Male	7 (28.6)	−1.566 to −0.0783	**0.0335**	19 (45.3)	−0.7641 to 0.0788	0.1154	37 (36.3)	−0.2418 to 0.1932	0.8249
Age	***Median value***	>67: 10 (58.8)	–	Reference	>64: 20 (55.5)	–	Reference	> 67: 49 (51.6)	–	Reference
		<67: 7 (41,2)	−0.02894 to 0.02794	0.9693	<64: 16 (44.4)	−0.0127 to 0.0207	0.6251	<67: 46 (48.4)	−0.0104 to 0,0128	0,8379

RNA-seq data performed on samples obtained by LUAD patients were used and analyzed by means of Lung Cancer Explorer [26,27]. LUAD patients (n = 321) were separated into 3 groups according to their smoking status: non-smokers (n = 32), smokers (n = 147) and former smokers (n = 142). In addition, where available, non-cancerous matched paired lung tissue was considered. In this latter case the number of samples were as follows: Non-Smoker: n = 7, Smoker: n = 19 and Former Smoker: n = 30. For each patient, gender, age at diagnosis, tumor stage and survival time were registered. RNA-seq expression values were normalized as log2 format to perform the analysis. The infiltration level of different immune cell populations was evaluated by TIMER2.0 (http://timer.cistrome.org/). In this study, we used CIBERSORT absolute (ABS), an analytical tool that allows the abundance of member cell types in a mixed cell population to be estimated using gene expression data [28].

2.11. Gene set enrichment analysis (GSEA) analysis

Gene set enrichment analysis (GSEA) was applied to identify significant gene sets between two groups which were defined as AIM2 positive or negative according to receiver operating characteristic (ROC) analysis, which allowed to identify a cut-off value according to the values of sensitivity and 1-specificity as in the area under the curve (AUC) analysis. All analyses were performed using GSEA v4.3.2 software (Broad Institute) using 'h.all.v2022.1.Hs.symbols.gmt' (Hallmark gene set) as reference database (https://www.gsea-msigdb.org/gsea/msigdb/human/genesets.jsp?collection=H). Significantly enriched gene sets were defined using a False Discovery Rate (FDR) q-value < 0.05 and a nominal p value < 0.05.

2.12. Differentially expressed genes analysis

The evaluation of the differentially expressed genes (DEGs) networks in LUAD patients with high transcriptional levels of AIM2 was analyzed via STRING database (version 11.5; string-db.org/) taking into consideration a high confidence score (<0.7). Biological processes evaluation associated to DEGs was performed through Gene ontology analysis. Gene network significance was evaluated by means of FDR approach (FDR significance threshold was set at 5 %) following Benjamini, Krieger and Yekutieli methods. Genes with an adjusted p-value less than 0.05 and a FDR greater than 1 were selected as DEGs between AIM2 positive and negative tumor tissues.

2.13. Statistical analysis

Data are presented as scatter dot plots showing the median. Statistical differences were assessed by means of two-tailed Wilcoxon matched-paired *t*-test and Mann Whitney *t*-test where appropriate. To discriminate the role of each single gene on clinical outcomes, ROC analysis was performed to extrapolate a cut-off value from the AUC. Percent survival was estimated using Kaplan-Meier method and compared with a non-parametric log-rank test. Statistical differences were evaluated according to Gehan-Breslow-Wilcoxon test. P values < 0.05 were considered significant. Statistical analysis was performed by using GraphPad prism 9.5.1 version (San Diego, USA).

3. Results

3.1. AIM2 mRNA is highly expressed in tumor tissues of LUAD patients

To evaluate the role of the AIM2 inflammasomes in the tumor tissue of LUAD patients, we used the public Cancer Genome Atlas TCGA_LUAD-2016 database.

Patients were differentiated according to the smoking history. The transcription of AIM2 mRNA was significantly higher in the tumor mass of Non-Smoker (Fig. 1a), Smoker (Fig. 1b) and Former Smoker (Fig. 1c) LUAD patients compared to healthy adjacent, non-tumor, tissues. Comparing the three groups of LUAD patients (Table 2), AIM2 transcripts were similarly higher in the tumor tissue despite the smoking status (LUAD Non-Smoker AIM2 median: 0.8125 read counts; LUAD Smoker AIM2 median: 1.017 read counts; LUAD Former Smoker AIM2 median: 0.9782 read counts). The expression of AIM2 was similar in non-cancerous tissues of Non-Smoker (median = 0.5939 read counts), Smokers (median = 0.4882 read counts) and Former Smokers (median = 0.5307 read counts) (Table 2).

Similarly, the transcription of AIM2 was evaluated based on the TNM stage. Tumor tissues of Non-Smoker LUAD patients had a significant increase of mRNA AIM2 at stage II (Fig. 1d). Instead, the levels of mRNA were higher at stage III and IV of Smoker LUAD patients compared to stage I and II (Fig. 1e). Former Smoker LUAD patients had significantly higher mRNA AIM2 starting from stage I up to stage IV (Fig. 1f). According to the non-homogenous expression of AIM2 in each group of patients, to define patients who were positive or not to AIM2 expression compared to the healthy non-tumor tissues, we performed a ROC analysis to extrapolate a cut-off value for each group of patients in order to stratify patients as expressing high or low levels of AIM2 (Supplementary Fig. S1a–c) (Table 3).

No statistical difference was found in terms of survival rate by

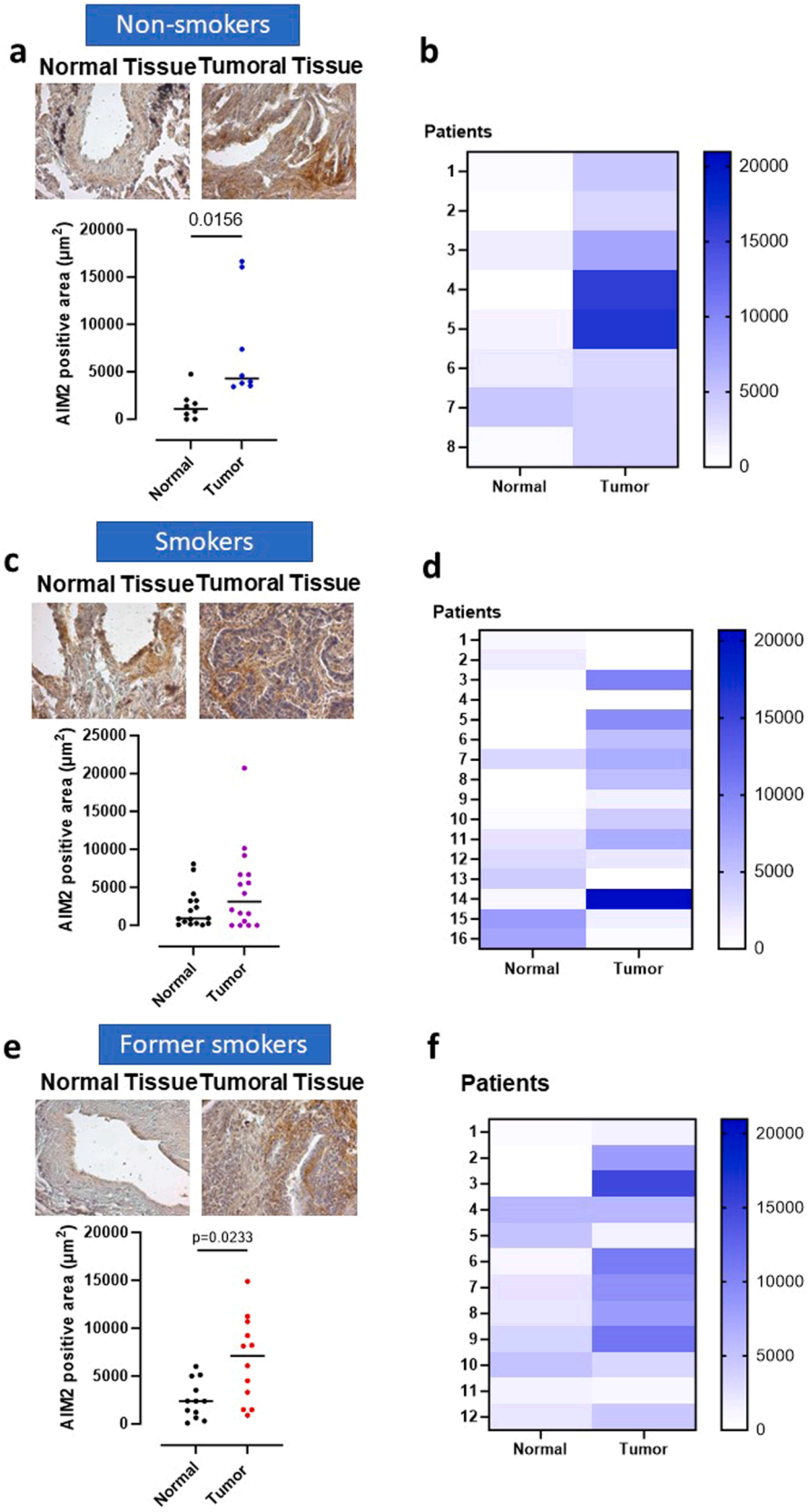

(caption on next page)

Fig. 2. Tumoral tissues of LUAD with different smoking status patients are characterized by high levels of AIM2. (**a**) Immunohistochemical analysis of AIM2 on normal and tumor matched tissues of Non-Smoker LUAD patients (n = 8) and AIM2 quantification in non-tumor (normal) and tumor tissues. (**b**) Heatmap showing increased AIM2 expression in tumor compared to normal tissues of Non-Smoker patients. (**c**) Immunohistochemical analysis of AIM2 on normal and tumor matched tissues of Smoker LUAD patients (n = 16) and AIM2 quantification in normal and tumor tissues. (**d**) Heatmap showing increased AIM2 expression in tumor compared to normal tissues of Smoker patients. (**e**) Immunohistochemical analysis of AIM2 on normal and tumor matched tissues of Former Smoker LUAD patients (n = 12) and AIM2 quantification in normal and tumor tissues. (**f**) Heatmap showing increased AIM2 expression in tumor compared to normal tissues of Former Smoker patients. Data in Fig. 1a–c are median, represented as scatter dot plots; statistical differences were assessed by means of two-tailed Wilcoxon matched-pairs signed rank test.

comparing high (median survival = 13 months, n = 17) versus low expression (median survival = 36 months, n = 10) of AIM2 mRNA in lung tissues of Non-Smoker patients (Fig. 1g). However, it has to be noted that 17 out of 27 (63 %) Non-Smoker patients survived less and were positive to AIM2, as confirmed by the hazard ratio (HR) of 1.7 (Fig. 1g, blue vs black line, p = 0.1722; Table 4). In particular, these patients had a Stage I LUAD (11 out of 17, 64 %), implying that higher transcriptional levels of AIM2 at early stage of LUAD had a negative impact on the prognosis of patients who have never smoked.

Smoker LUAD patients who were expressing higher levels of AIM2 had lower survival rate than patients with lower levels (Fig. 1h, purple vs black line, median survival = 12 vs 86 months, respectively). To note, 109 out of 138 (79 %) Smoker LUAD patients expressed higher levels of AIM2 (Fig. 1h). Similarly, Former Smoker patients with high AIM2 expression had a poorer survival rate than patients with lower AIM2 levels (Fig. 1i, red vs black line, median survival = 20 vs 49 months, respectively). In this group, patients with high levels of AIM2 were 94 out of 134 (67 %) patients. To note, Smoker LUAD patients with high AIM2 levels had a HR of 3.3 (Table 4) and Former Smokers with high AIM2 levels had a HR of 2.3 (Table 4), further confirming that AIM2 is involved in LUAD progression [6].

Moreover, we performed a multivariate analysis of AIM2 + samples compared to other clinical variables (where available), such as stage, oncogene mutation, sex and age. As reported in Table 5, higher expression of AIM2 in the tumor tissue is correlated to Stage II and sex in Non-Smoker LUAD patients. No other significant differences were noted, most likely because of the low number of samples that had the required information. Thus, a bigger dataset would be needed to make conclusions.

To validate the transcriptomic data, we evaluated the protein levels of the AIM2 inflammasome in LUAD patients from GLAD study [22]. We found that both Non-Smokers (Fig. 2a and b) and Former Smokers (Fig. 2e and f) had significant higher levels of AIM2 in the tumor mass than the non-cancerous (normal) tissues. Instead, Smokers still had a tendency of higher AIM2 expression in the tumor mass than normal tissues, although the difference did not reach statistical differences (Fig. 2c and d).

Together these data (protein and mRNA levels) strongly support the involvement of AIM2 that is associated to poor prognosis of LUAD patients despite the smoking status.

3.2. *Higher AIM2 levels are associated to the recruitment of non-activated DCs and T cells in the lung of LUAD patients and former smoking mice*

To investigate the cellular mechanism by which high expression of AIM2 drives LUAD progression and poor prognosis, we analyzed tumor immune cell infiltration by taking advantage of CIBERSORT-ABS algorithm which, according to a gene signature matrix containing 547 genes, allows the identification of 22 immune cell subsets [28].

The deconvolution of gene expression data of Non-Smoker LUAD patients did not provide any information on the cellular composition of this group (data not shown), maybe due to the fact that the algorithm was not able to characterize and to quantify each immune cell subtype according to the available number of patients.

Instead, we found no differences in terms of activated (Fig. 3a) and resting (Fig. 3c) myeloid DCs (mDCs) in both AIM2 + and AIM2- Smoker LUAD patients. Instead, AIM2 + Former Smoker LUAD patients had significantly lower activated mDCs (Fig. 3b), but higher levels of resting mDCs (Fig. 3d). It has to be pointed out that, according to the CIBERSORT analysis, the differences between resting and activated mDCs were defined by unique gene signatures and that some genes were included in both cell types [28]. Activated mDCs were characterized by higher expression of genes involved in the positive regulation of antigen processing and presentation (i.e. CCL19 and CCR7), DC differentiation and chemotaxis (i.e. CCL5). Instead, these genes were missing in the resting mDCs-associated gene signature. Moreover, Treg were not altered in Smoker LUAD patients (Supplementary Fig. S2a), differently than Former Smokers (Supplementary Fig. S2b). CD8 + T cells were no differently present in both groups (Supplementary Fig. S2c and d); instead, while NK cells in their resting status were significantly higher and activated NK cells did not show any difference in Smoker LUAD tissues (Supplementary Fig. S2e and g), they were significantly reduced in Former Smoker LUAD patients (Supplementary Fig. S2f and S2h).

To confirm the role of recruited DCs and immunosuppressive T cell environment into the lung of Former Smoker patients, we took advantage of a mouse model of smoking mice [6]. Former smoking mice were exposed to smoking for 4 weeks and then to room air for 16 weeks. In our previous study [6], we already found that first-hand cigarette smoking induced lung inflammation and increased the infiltration of AIM2 positive DCs [6]. In this set of experiments, we found that similar to smoking mice, former smoking mice had higher mean linear intercept (MLI) (Fig. 4a), but did not have mucus production characterized by PAS positive staining (Supplementary Fig. S3a), as well as no deposition of collagen (Supplementary Fig. S3b). No differences in terms of infiltrated macrophages (Supplementary Fig. S3c), myeloid-derived suppressor cells (MDSC, identified as CD11b + Gr-1 + cells) (Supplementary Fig. S3d) and AIM2 + macrophages (Supplementary Fig. S3e) were observed. These data were similar to what observed for TCGA-LUAD 2016 (Fig. 3 and Supplementary Fig. S2).

The analysis of the infiltration of immune cells to the lung of former smoking mice was characterized by Treg (identified as CD4 + CD25 + FoxP3 + cells) (Fig. 4b), DCs (identified as CD11c high CD11b int cells) (Fig. 4c), which were not active as MHC II was not overexpressed compared to room air-exposed mice (Fig. 4d). Instead, we found that lung infiltrated DCs in Former Smoker mice had higher expression of AIM2 than those observed in the lungs of Room Air-exposed mice (Fig. 4e, green vs black dots).

It is well-known that cigarette smoking models the immune landscape by promoting the release of cytokines and chemokines that drive to the recruitment of immune cells to the lung. Previously, we found that the lung of cigarette smoking mice had higher levels of AIM2-dependent inflammasome cytokines, such as IL-1α, IL-1β, IL-18 and IL-33 associated to the immunosuppressive IL-10 [6]. Similarly, in the lung of former smoking mice, higher levels of IL-1α (Fig. 4f), IL-1β (Fig. 4g), IL-33 (Fig. 4h) and the immunosuppressive TGF-β (Fig. 4i) were detected than Room-exposed mice. However, IL-18 (Supplementary Fig. S3f), TNF-α (Supplementary Fig. S3g) and LDH (Supplementary Fig. S3h) were not different between former smoking and room-air-exposed mice.

Thus, this experimental mouse model showed that although smoking cessation switches off processes such as collagen deposition and mucus production, it is not able to revert smoke-induced emphysema-like features in mice, a condition that is associated with a tolerogenic and immunosuppressive lung microenvironment highly populated by Tregs and AIM2 positive DCs in a context of IL-1-based inflammation, similarly to what observed for LUAD samples.

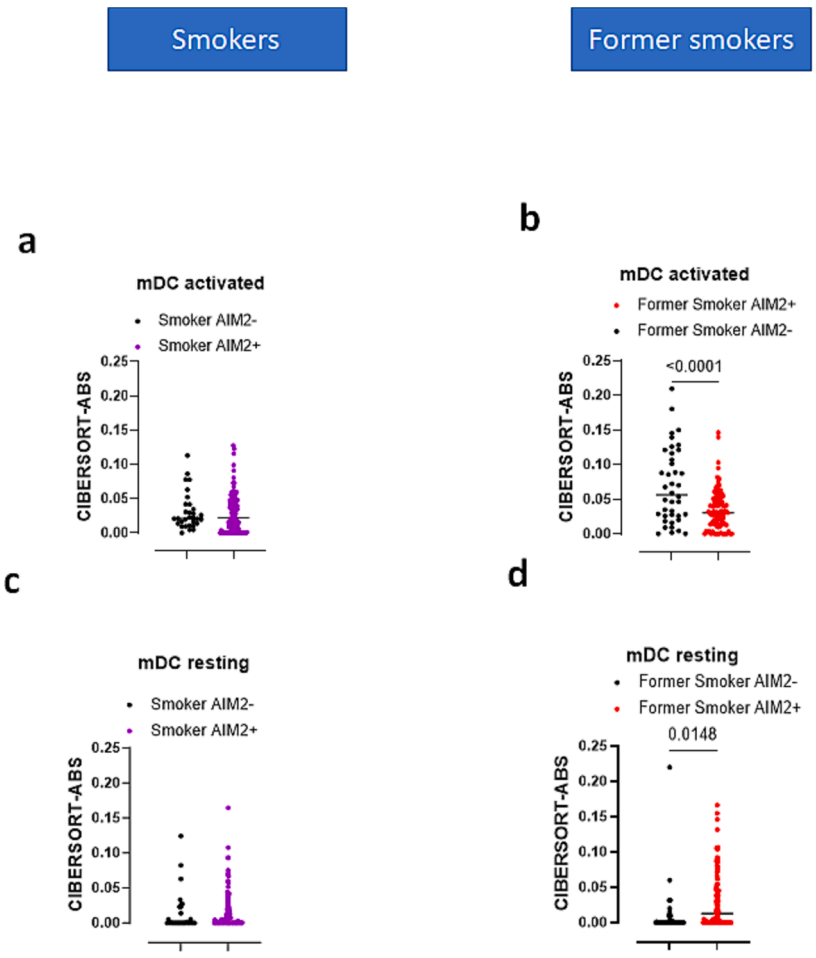

Figure 3

(caption on next page)

Fig. 3. Expression levels of DC subsets in tumor tissues of Smoker and Former Smoker patients according to the AIM2 mRNA expression. Scatter dot plot of the expression levels of myeloid dendritic cells (mDCs) in the activated status (**a**, **b**) and mDCs in the resting status (**c**, **d**) in the cancerous tissues of Smoker (**a**, **c**, n = 147) and Former Smoker patients (**b**, **d**, n = 142) according to the AIM2 transcriptional expression level (Smoker AIM2+, violet dots, n = 116; Smoker AIM2-,blak dots n = 31; Former Smoker AIM2+, red dots, n = 102; Former Smoker AIM2-, black dots, n = 40). Data are represented as median and scatter dot plots. Statistical analysis was performed using the Mann–Whitney *U* test.. (For interpretation of the references to colour in this figure legend, the reader is referred to the web version of this article.)

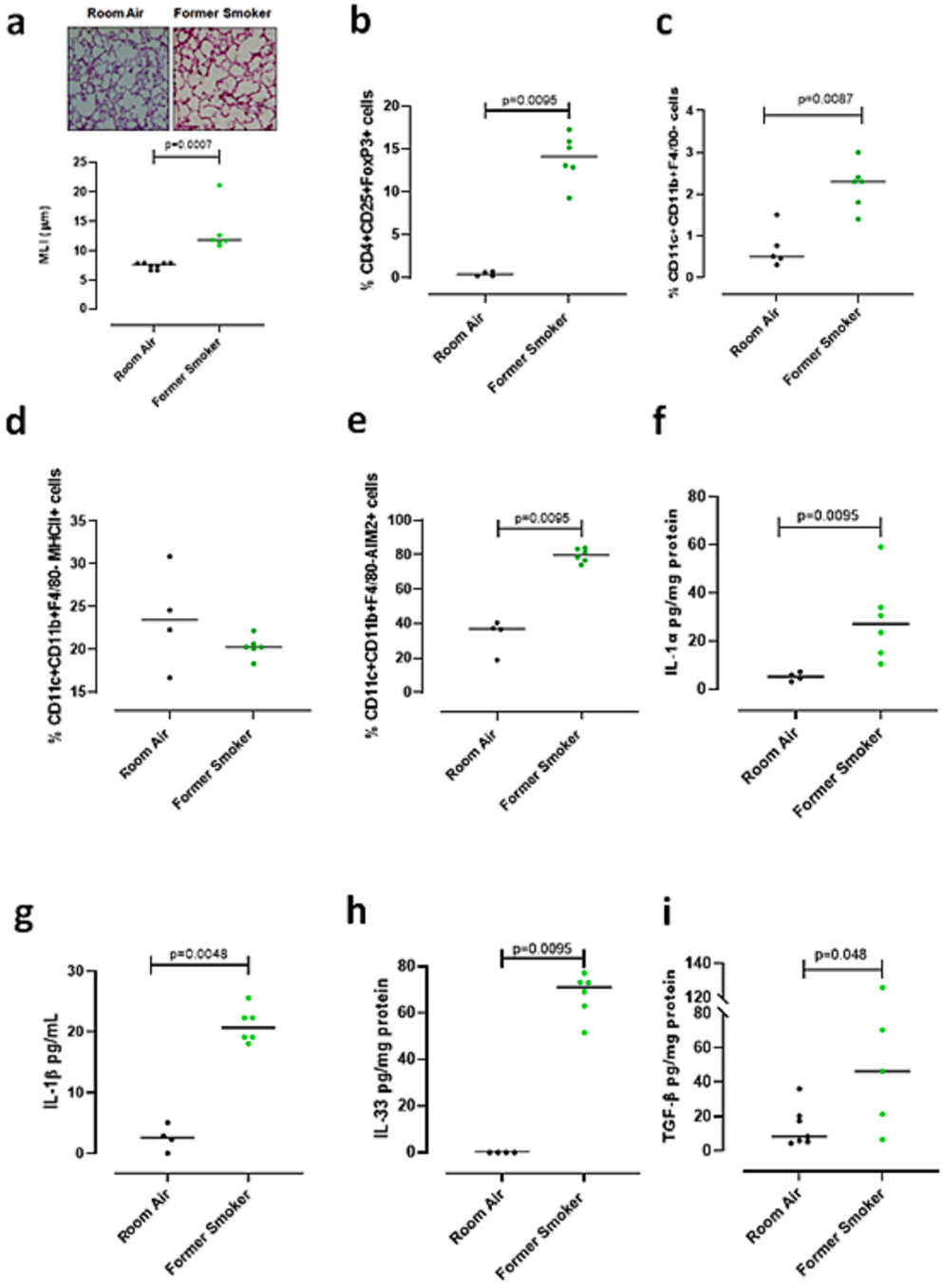

Fig. 4. Smoking cessation did not reverse cigarette smoke-induced emphysema-like alveolar enlargement in mice and it is associated to a lung immunosuppressive microenvironment.**a**) H&E staining on left lung lobe cryosections of Room Air-exposed and Former Smoker C57BL/6N mice and mean linear intercept (MLI) analysis performed by using ImageJ software (NIH, USA). Lungs from former smoker mice were digested and flow cytometry was performed to identify regulatory T cells (Treg) (**b**) and dendritic cells (DCs) (**c**). The expression of MHC II (**d**) and intracellular AIM2 (**e**) was assessed on lung recruited DCs. The levels of IL-1α (**f**), IL-1β (**g**), IL-33 (**h**) and TGF-β (**i**) were assessed. IL-1α (**f**), IL-33 (**h**) and TGF-β (**i**) were assessed in lung homogenates, whereas IL-1β (**g**) was assessed in BAL samples obtained by Room Air (black dots) and Former Smoker mice (green dots). Statistical analysis was performed using the Mann–Whitney *U* test. Experiments were repeated twice with n = 4–8 mice/group. (For interpretation of the references to colour in this figure legend, the reader is referred to the web version of this article.)

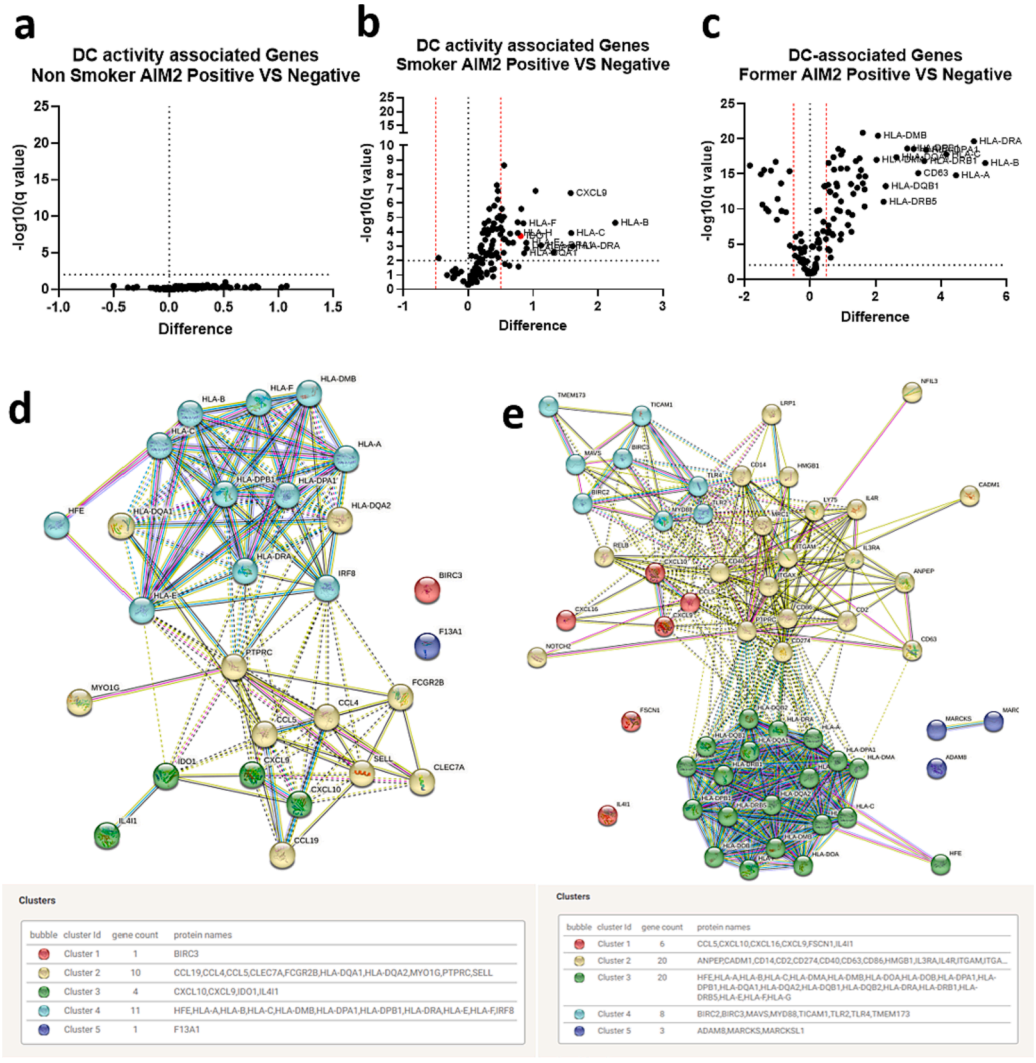

(caption on next page)

Fig. 5. Biological processes associated to 'dendritic cells activity' in Non-Smoker, Smoker and Former Smoker LUAD Patients with high levels of AIM2 mRNA in the cancerous tissues. Volcano plots showing differentially expressed genes associated to dendritic cells (DCs) activity in Non-Smoker (**a**), Smoker (**b**) and Former Smoker (**c**) LUAD patients with high (positive) versus low (negative) transcriptional level of AIM2. Black dots in the upper right quadrant of each volcano plot indicate upregulated genes in LUAD Patients with high expression of AIM2. STRING network of the 27 differentially expressed genes (DEGs) associated to DCs activity in AIM2 positive Smoker LUAD patients (**d**). STRING network of the 57 DEGs associated to DCs activity in AIM2 positive Former Smoker LUAD patients (**e**). Bubble graphs showed the biological processes associated to a network of DEGs associated to DCs activity in Smoker (**f**) and Former Smoker (**g**) LUAD patients. For bubble graphs, the number (N) of connecting genes was allocated to the x-axis and the network strength between genes to y-axis. The region of bubbles is proportional to the number of connecting genes in a network and associated to the biological process. Data in Fig. a–c were analyzed by using the multiple unpaired *t*-test and FDR approach (Benjamini, Krieger, and Yekutieli method) to adjust the p-values. The genes with adjusted p-value less than 0.05 and FDR greater than 1 were selected as differentially expressed genes.

3.3. Genes associated to DCs activity in AIM2 positive LUAD patients

According to previous data (Figs. 3 and 4), we focused our attention on DCs population. Therefore, we investigated the profile of gene expression associated to 'DCs activity' in AIM2 positive vs AIM2 negative Non-Smoker, Smoker and Former Smoker LUAD patients.

The analysis of genes associated to 'DCs activity' revealed that no gene was differentially expressed in AIM2 positive vs AIM2 negative Non-smoker LUAD patients (Fig. 5a). Instead, AIM2 positive had 70 upregulated and 1 down-regulated (CD14) DC-related genes compared to AIM2 Negative Smoker LUAD patients (Fig. 5b, Table 6). Among the upregulated genes, HLA family proteins, IDO1, BIRC3, CXCL9, CXCL10, and others (STRING dataset, Fig. 5d), highlighted that an immunosuppressive phenotype of DCs were more likely present in the tumor tissue of smoker LUAD patients, similarly to what observed for smoking mice [6]. When we analyzed DC-related genes in AIM2 Positive vs AIM2 Negative Former Smokers we found that 74 DC-related genes were upregulated (Table 7) and 32 downregulated in AIM2 positive patients compared to AIM2 Negative LUAD patients (Fig. 5c). Again, STRING analysis was performed, and we found that similar genes as smoker LUAD patients were expressed in this cohort of patients, except for ADAM8, BIRC2 and BIRC3, CD274, which were upregulated in AIM2 Positive Former Smoker LUAD patients (Fig. 5e). To note, the difference between AIM2 Positive Smoker vs Former Smoker LUAD patients was mainly related to TLR2, TLR4 and STING (TMEM173) gene expression (Fig. 5d vs e). To delineate the molecular interactions and pathways associated to DC-related upregulated genes in AIM2 Positive Smoker LUAD patients, we used the same analytical approach and found that 10 biological processes had higher FDR and network strength (Table 8, Fig. 5f), which reconducted toward an immunosuppressive environment as previously observed (Fig. 3 and [6]). Similarly, AIM2 Positive Former Smoker LUAD patients were characterized by 8 biological processes with high FDR and network strength (Table 9, Fig. 5g), which again reflected an immunosuppressive profile. We also observed that in both Smoker and Former Smoker LUAD patients who were AIM2 positive were characterized by genes associated to common biological processes, as inflammatory response, response to cytokines and Toll-like receptor (TLR)-signaling pathways (Fig. 5f, g and Tables 8 and 9). Although similar pathways related to cytokines response and inflammation (i.e. NF-kappa B signaling pathway, NOD-like receptor signaling pathway, regulation of IL-1 production, Tumor-necrosis factor signaling pathway etc.) were found in AIM2 + Smoker and Former Smoker patients, we observed that among the genes associated to the cytosolic dsDNA sensing, TMEM173 was upregulated in the sole AIM2 + Former Smoker patients, implying that inflammasome-independent function of AIM2 could occur in LUAD patients who stopped smoking.

All together these results imply that high expression of AIM2 in LUAD patients, beyond their smoking history, underlies an increased number of resting mDCs which have an immunosuppressive phenotype.

To better investigate how the AIM2 profile was involved into LUAD development and progression, we went on by analyzing gene expression data by using Gene set enrichment analysis (GSEA). We found that upregulated hallmark gene sets were 15 in Non-Smoker (Fig. 6a), 19 in Smoker (Fig. 6b) and 33 in Former Smoker (Fig. 6c) LUAD patients with higher expression of AIM2. Among these, 13 processes were in common within the three groups of AIM2 + LUAD patients (Fig. 6d), all related to tumor growth.

Among biological processes, we took into consideration the role of AIM2 in increasing the inflammatory response. We found that the enrichment score for Non-Smoker AIM2 positive versus AIM2 negative LUAD patients was of 0.4 (Fig. 7a); instead for Smoker AIM2 positive versus AIM2 negative LUAD patients it was of 0.7 (Fig. 7d) and for Former Smoker AIM2 positive versus AIM2 negative LUAD patients it was of 0.35 (Fig. 7g), leading to think that AIM2 positive Non-Smoker LUAD patients were biologically similar to AIM2 positive Former Smokers compared to Smokers. Though, the enriched processes in Former Smokers were higher (n = 33 upregulated hallmark gene sets) (Fig. 6c) than the other two groups (Fig. 6a and b). We then went into the GSEA data and performed ROC analysis for the upregulated genes in the three groups regarding the inflammatory response-related genes, in order to create an inflammatory profile (Tables 10, 11 and 12). Specifically, for each upregulated gene, the ROC analysis was performed by comparing the gene expression in AIM2 Negative versus AIM2 Positive patients. To identify the inflammation-dependent transcriptomic profile we took into consideration the sole genes who reached a value of AUC of 0.8 (Tables 10, 11 and 12, refer to italics). We defined two transcriptomic profiles as follows: 1. Positive Inflammatory Profile, that characterized patients who were positive to AIM2 and who had higher expression of at least 80 % of the selected genes (according to the chosen cut-off); 2. Negative Inflammatory Profile, that characterized patients with higher expression of AIM2 and with lower expression of the selected genes (below the cut-off as from the AUC). Non-Smoker patients who were positive to AIM2 and to the inflammatory profile had lower survival rate (n = 13, median survival = 13 months) than AIM2 positive but negative to the inflammatory profile 1 (n = 3, median survival = undefined) (Fig. 7b, red vs black line). Similarly, Smoker AIM2 positive LUAD patients who were positive to the inflammatory profile 1, had lower survival rate (n = 81, median survival = 14 months) than AIM2 positive but were negative to the inflammatory profile (n = 28, median survival = 56 months) (Fig. 7e, red vs black line). Double positive AIM2 and inflammatory profile Former Smokers had a significant lower survival rate (n = 60, median survival = 24 months) than AIM2 positive but negative to the inflammatory profile (n = 34, median survival = 40 months) (Fig. 7h, red vs black lines).

Because AIM2 is a receptor of the inflammasome complex, we went on by discriminating the survival rate according to the expression of CASP1, IL1B, IL18 and IL1A. In order to create an inflammasome gene signature correlated to the outcomes of LUAD patients with different smoking status, we applied the same analytic approach as above. We established two transcriptomic profiles to assess the prognosis of each patient as follows: 1. Positive Inflammasome Profile: patients with high expression of AIM2 and with higher expression of at least 3 out of 4 genes (CASP1, IL1B, IL18, IL1A), according to the AUC-derived cut-off; 2. Negative Inflammasome Profile: patients with higher expression of AIM2 and with higher expression of less than 3 out of 4 genes (CASP1, IL1B, IL18, IL1A). We found no differences in terms of survival rate for Non-Smoker (Fig. 7c, red vs black line) and Smoker LUAD patients according to the positivity or negativity to the inflammasome profile (Fig. 7f, red vs black line). Instead, Former Smoker LUAD patients who were positive to the inflammasome profile survived more (n = 28,

Table 6
DCs activity-associated genes upregulated in Smoker LUAD patients with high expression of AIM2 in the tumoral tissues.

	P value	Mean of Smoker AIM2+	Mean of Smoker AIM2-	Difference	SE of difference	t ratio	df	q value
CCL4	<0,000001	1.477	0.9247	0.5527	0.07725	7.154	145	<0,000001
PDCD1LG2	<0,000001	1.207	0.7665	0.4404	0.06865	6.416	145	<0,000001
CXCL10	<0,000001	2.291	1.255	1.036	0.1694	6.117	145	<0,000001
IL2RA	<0,000001	1.295	0.8389	0.456	0.07476	6.099	145	<0,000001
CXCL9	<0,000001	3.195	1.615	1.58	0.2638	5.988	145	<0,000001
CD86	<0,000001	1.79	1.336	0.4546	0.07927	5.734	145	<0,000001
TLR8	<0,000001	1.27	0.8683	0.4017	0.07319	5.489	145	0.000002
IRF8	<0,000001	1.892	1.376	0.5163	0.09641	5.355	145	0.000002
TLR7	<0,000001	1.193	0.8684	0.3247	0.06096	5.326	145	0.000002
CCL5	<0,000001	2.497	1.681	0.8156	0.1536	5.31	145	0.000002
CD2	0.000001	1.734	1.248	0.4859	0.09652	5.035	145	0.000008
IL4I1	0.000002	1.747	1.199	0.5483	0.11	4.986	145	0.000009
FCGR2B	0.000002	1.89	1.359	0.5306	0.1076	4.932	145	0.00001
CD274	0.000002	1.135	0.6842	0.4506	0.09181	4.908	145	0.000011
CLEC7A	0.000004	1.835	1.322	0.5122	0.1065	4.81	145	0.000015
CCR2	0.000004	1.215	0.9029	0.312	0.06543	4.768	145	0.000017
PTPRC	0.000006	2.833	2.073	0.7604	0.1617	4.701	145	0.000022
HLA-B	0.000007	9.246	6.981	2.265	0.485	4.669	145	0.000023
HLA-F	0.000008	3.229	2.38	0.8489	0.183	4.64	145	0.000025
CXCR3	0.000009	1.166	0.7705	0.396	0.08596	4.607	145	0.000026
CD80	0.000009	0.8595	0.6066	0.2529	0.05501	4.598	145	0.000026
SIRPA	0.000019	2.662	2.163	0.4989	0.1128	4.423	145	0.00005
CD7	0.00002	1.468	1.09	0.3776	0.08551	4.416	145	0.00005
CD209	0.000026	1.453	1.012	0.4405	0.1013	4.349	145	0.000063
C1orf54	0.000029	1.182	0.9286	0.2535	0.05873	4.316	145	0.000069
TRAF1	0.000031	1.72	1.421	0.2988	0.06942	4.305	145	0.000069
TLR4	0.000032	1.811	1.44	0.371	0.0864	4.294	145	0.000069
CLEC10A	0.000033	1.253	0.881	0.3722	0.08677	4.289	145	0.000069
TLR1	0.000035	1.467	1.211	0.2554	0.05977	4.273	145	0.000071
SELL	0.000041	1.733	1.211	0.5215	0.1232	4.233	145	0.000081
HLA-H	0.000063	3.792	3.028	0.7637	0.1853	4.121	145	0.000121
HLA-C	0.000066	7.986	6.401	1.585	0.3857	4.111	145	0.000121
TLR10	0.000069	0.9019	0.5951	0.3068	0.07483	4.1	145	0.000121
CGAS	0.000069	1.232	1.009	0.2228	0.05434	4.099	145	0.000121
BIRC3	0.000077	2.46	1.814	0.6453	0.1585	4.071	145	0.000131
IRF4	0.000089	1.53	1.035	0.4944	0.1226	4.031	145	0.000147
CD5	0.000091	1.329	1.032	0.2967	0.07367	4.027	145	0.000147
IDO1	0.000123	2.259	1.45	0.8082	0.2048	3.946	145	0.000195
CCL19	0.000201	1.618	1.072	0.5462	0.1432	3.816	145	0.000309
MYO1G	0.000228	2.051	1.485	0.5656	0.1496	3.78	145	0.000343
NAAA	0.000242	1.787	1.526	0.261	0.06932	3.765	145	0.000354
FAS	0.000294	1.881	1.498	0.3828	0.1031	3.711	145	0.000421
HLA-DMB	0.000407	3.189	2.498	0.6905	0.1908	3.619	145	0.00057
HLA-E	0.000421	5.707	4.813	0.8943	0.2478	3.61	145	0.000577
HLA-DQA2	0.000434	2.197	1.577	0.6196	0.172	3.601	145	0.000582
CD40	0.000593	2.097	1.728	0.3687	0.105	3.512	145	0.000778
HLA-DPA1	0.000696	5.361	4.238	1.123	0.324	3.466	145	0.000876
CD33	0.000697	1.074	0.8706	0.2033	0.05867	3.465	145	0.000876
HLA-DRA	0.000797	7.74	6.131	1.609	0.4696	3.426	145	0.000982
CLEC6A	0.000996	0.443	0.2557	0.1873	0.05573	3.36	145	0.001203
HLA-DPB1	0.001192	4.472	3.573	0.8984	0.2717	3.306	145	0.001412
LY75	0.001278	2.132	1.775	0.3562	0.1084	3.285	145	0.001486
SOCS1	0.001473	1.223	1.034	0.1888	0.05824	3.242	145	0.00168
RELB	0.002115	1.921	1.691	0.2295	0.07331	3.13	145	0.002369
CD200	0.002454	1.353	1.148	0.2051	0.06652	3.083	145	0.002682
HLA-A	0.002482	8.37	7.055	1.314	0.4268	3.079	145	0.002682
F13A1	0.00265	2.433	1.887	0.546	0.1785	3.059	145	0.002815
ITGAX	0.002698	2.091	1.779	0.3121	0.1022	3.053	145	0.002817
MARCKS	0.002796	3.709	3.274	0.4347	0.1429	3.041	145	0.002871
HLA-DQA1	0.002987	3.64	2.778	0.8613	0.2852	3.02	145	0.003016
HLA-DRB6	0.003365	2.086	1.664	0.4221	0.1416	2.982	145	0.003344
ITGAM	0.004056	1.963	1.6	0.3632	0.1244	2.92	145	0.003966
CLEC12A	0.004424	0.9674	0.6922	0.2752	0.09516	2.892	145	0.004259
CCR7	0.004747	1.225	0.8501	0.3753	0.1309	2.868	145	0.004499
HLA-G	0.005042	1.313	0.9624	0.351	0.1233	2.848	145	0.004607
CLEC4C	0.005084	0.287	0.2377	0.04928	0.01732	2.845	145	0.004607
TLR6	0.00585	0.8687	0.7507	0.1181	0.04221	2.797	145	0.005224
HLA-DOA	0.006698	2.484	2.023	0.4604	0.1674	2.751	145	0.005895
MYD88	0.008547	2.737	2.554	0.1829	0.06859	2.666	145	0.007313
CD83	0.009749	1.848	1.63	0.2182	0.0833	2.619	145	0.008228

Table 7
Dendritic cells (DCs) activity-associated genes upregulated in Former Smoker LUAD patients with high expression of AIM2 in the tumoral tissues.

	P value	Mean of Former Smoker AIM2+	Mean of Former Smoker AIM2-	Difference	SE of difference	t ratio	df	q value	-log10 (q value)
PTPRC	<0,000001	2.838	1.228	1.61	0.1351	11.91	140	<0,000001	20.86
HLA-DMB	<0,000001	3.359	1.287	2.072	0.178	11.64	140	<0,000001	20.45
HLA-DRA	<0,000001	8.231	3.236	4.996	0.4435	11.27	140	<0,000001	19.66
HLA-DPB1	<0,000001	4.845	1.879	2.966	0.274	10.82	140	<0,000001	18.64
HLA-E	<0,000001	5.721	2.558	3.163	0.2943	10.75	140	<0,000001	18.55
CD2	<0,000001	1.772	0.9012	0.8706	0.08121	10.72	140	<0,000001	18.55
HLA-DPA1	<0,000001	5.804	2.261	3.543	0.3329	10.64	140	<0,000001	18.41
IL4I1	<0,000001	1.634	0.642	0.9922	0.09396	10.56	140	<0,000001	18.26
HLA-C	<0,000001	7.675	3.518	4.157	0.4011	10.36	140	<0,000001	17.81
CD40	<0,000001	2.058	1.105	0.9529	0.09227	10.33	140	<0,000001	17.76
HLA-DQA1	<0,000001	3.995	1.361	2.634	0.2593	10.16	140	<0,000001	17.39
CD86	<0,000001	1.773	1.055	0.7182	0.07073	10.15	140	<0,000001	17.39
ADAM8	<0,000001	2.528	1.02	1.507	0.1497	10.07	140	<0,000001	17.22
HLA-DMA	<0,000001	3.633	1.602	2.031	0.2035	9.981	140	<0,000001	17.02
HLA-DRB1	<0,000001	5.647	2.16	3.488	0.3522	9.902	140	<0,000001	16.84
IL4R	<0,000001	2.984	1.585	1.399	0.1415	9.882	140	<0,000001	16.82
IL3RA	<0,000001	1.228	0.6597	0.5679	0.05822	9.755	140	<0,000001	16.55
HLA-B	<0,000001	9.107	3.764	5.343	0.5481	9.748	140	<0,000001	16.55
ITGAX	<0,000001	2.087	1.146	0.9404	0.09974	9.428	140	<0,000001	15.79
BIRC2	<0,000001	2.506	1.376	1.13	0.1201	9.411	140	<0,000001	15.76
HLA-DOB	<0,000001	1.332	0.6001	0.7324	0.07835	9.348	140	<0,000001	15.62
HLA-DOA	<0,000001	2.706	1.154	1.553	0.1668	9.307	140	<0,000001	15.54
CD63	<0,000001	6.883	3.581	3.302	0.3624	9.111	140	<0,000001	15.11
HLA-A	<0,000001	8.315	3.862	4.452	0.4961	8.974	140	<0,000001	14.8
HMGB1	<0,000001	4.086	2.587	1.499	0.1682	8.909	140	<0,000001	14.65
NOTCH2	<0,000001	3.769	2.089	1.68	0.1887	8.902	140	<0,000001	14.65
HLA-F	<0,000001	3.198	1.587	1.611	0.1897	8.496	140	<0,000001	13.66
TICAM1	<0,000001	1.896	1.087	0.8081	0.09531	8.479	140	<0,000001	13.63
MARCKS	<0,000001	3.535	2.285	1.25	0.1481	8.439	140	<0,000001	13.55
CD274	<0,000001	0.9901	0.4383	0.5519	0.06573	8.397	140	<0,000001	13.46
PDCD1LG2	<0,000001	1.123	0.646	0.4772	0.05732	8.325	140	<0,000001	13.29
HLA-DQB1	<0,000001	4.349	2.039	2.31	0.2782	8.304	140	<0,000001	13.25
LY75	<0,000001	2.169	1.338	0.83	0.1001	8.293	140	<0,000001	13.24
CGAS	<0,000001	1.095	0.6569	0.4383	0.05286	8.29	140	<0,000001	13.24
HLA-DQA2	<0,000001	2.379	0.9373	1.442	0.1759	8.198	140	<0,000001	13.02
FSCN1	<0,000001	2.961	1.296	1.665	0.2057	8.094	140	<0,000001	12.78
TLR4	<0,000001	1.805	1.207	0.5979	0.07493	7.979	140	<0,000001	12.51
RELB	<0,000001	1.939	1.317	0.6218	0.0783	7.941	140	<0,000001	12.43
BIRC3	<0,000001	2.627	1.306	1.321	0.1687	7.829	140	<0,000001	12.17
NFIL3	<0,000001	2.118	1.336	0.782	0.1011	7.737	140	<0,000001	11.96
TLR2	<0,000001	2.354	1.412	0.9426	0.128	7.362	140	<0,000001	11.09
HLA-DRB5	<0,000001	3.83	1.584	2.246	0.3061	7.338	140	<0,000001	11.04
LRP1	<0,000001	4.665	2.998	1.667	0.237	7.033	140	<0,000001	10.35
STING1	<0,000001	2.821	1.993	0.8283	0.1213	6.826	140	<0,000001	9.895
HLA-L	<0,000001	0.8123	0.5315	0.2808	0.04135	6.792	140	<0,000001	9.825
HLA-DPB2	<0,000001	0.5546	0.339	0.2156	0.03198	6.742	140	<0,000001	9.728
CXCL10	<0,000001	2.04	1.126	0.914	0.1356	6.741	140	<0,000001	9.728
HLA-H	<0,000001	3.641	2.474	1.166	0.1757	6.638	140	<0,000001	9.53
CD14	<0,000001	4.817	3.525	1.292	0.1998	6.468	140	<0,000001	9.158
MAVS	<0,000001	3.014	2.292	0.7226	0.1163	6.216	140	<0,000001	8.614
CD5	<0,000001	1.349	0.937	0.4124	0.06878	5.996	140	<0,000001	8.154
CADM1	<0,000001	2.796	1.639	1.157	0.1999	5.789	140	<0,000001	7.727
HLA-G	<0,000001	1.318	0.7563	0.5619	0.09748	5.764	140	<0,000001	7.679
MYD88	<0,000001	2.864	2.293	0.5717	0.1067	5.359	140	<0,000001	6.862
CD1C	<0,000001	1.058	0.6548	0.4031	0.07535	5.35	140	<0,000001	6.85
HLA-DQB2	<0,000001	2.213	0.9481	1.265	0.2385	5.303	140	<0,000001	6.763
ITGAM	<0,000001	1.962	1.418	0.5439	0.1042	5.218	140	<0,000001	6.601
CCL5	<0,000001	2.459	1.787	0.6713	0.1306	5.141	140	<0,000001	6.463
TLR6	<0,000001	0.8419	0.6229	0.219	0.04278	5.12	140	<0,000001	6.427
ANPEP	0.000001	2.083	1.133	0.9502	0.1859	5.11	140	<0,000001	6.414
CXCL16	0.000001	3.514	2.813	0.7017	0.1393	5.038	140	<0,000001	6.28
THBD	0.000005	2.233	1.744	0.4888	0.1032	4.737	140	0.000002	5.725
CSF2	0.000007	0.613	0.3537	0.2594	0.05542	4.68	140	0.000002	5.628
MARCKSL1	0.000007	3.75	2.825	0.9251	0.1977	4.679	140	0.000002	5.628
TLR8	0.000018	1.214	0.9339	0.28	0.06307	4.44	140	0.000006	5.21
CD33	0.000018	1.108	0.877	0.2308	0.05202	4.436	140	0.000006	5.207
CLEC9A	0.000069	0.4145	0.3167	0.09778	0.02384	4.102	140	0.000023	4.643
CLEC4C	0.000072	0.2821	0.2213	0.06073	0.01485	4.09	140	0.000023	4.633
CD83	0.00013	1.919	1.637	0.2827	0.07181	3.936	140	0.00004	4.394
HLA-DRB6	0.000173	2.317	1.763	0.5535	0.1434	3.86	140	0.000052	4.28
MRC1	0.000267	2.635	2.035	0.5999	0.1604	3.74	140	0.00008	4.094
CXCL9	0.002895	2.836	2.204	0.6324	0.2086	3.032	140	0.000827	3.083
CD1E	0.003817	0.9005	0.6836	0.2169	0.07372	2.942	140	0.001079	2.967
BCL6	0.02242	2.702	2.532	0.1704	0.07379	2.309	140	0.005971	2.224

Table 8
Biological processes linked to 70 upregulated genes associated to Dendritic cells (DCs) activity in Smoker LUAD patients with high levels of AIM2.

Biological Process	Genes in the network	Network strength	FDR
Regulation of immune system process	HLA-A, HLA-B, HLA-E, HLA-F, HLA-DPB1, HLA-DQA1, HLA-DQA2, HLA-DMB, HLA-DRA, HFE, BIRC3, PTPRC, MYO1G, FCGR2B, CCL4, CCL5, IDO1, CLEC7A, SELL, CXCL10, CCL19	1.04	2.82e-18
Inflammatory response	CCL19, CCL4, CCL5, CCR2, CCR7, CD40, CLEC7A, CXCL10, CXCL9, CXCR3, FCGR2B, IDO1, IL2RA, ITGAM, LY75, MYD88, RELB, TLR1, TLR10, TLR4, TLR6, TLR7, TLR8	1.09	1.88e-16
Response to cytokines	BIRC3, CCL19, CCL4, CCL5, CCR2, CCR7, CD274, CD40, CXCL10, CXCL9, CXCR3, FAS, HLA-DPA1, IL2RA, IRF8, MYD88, RELB, SIRPA, SOCS1, TLR4, TRAF1	0.87	5.89e-11
Negative regulation of lymphocyte mediated immunity	HLA-A, HLA-B, HLA-E, HLA-F, HFE, PTPRC, FCGR2B	2.08	1.16e-10
Negative regulation of leukocytes mediated cytotoxicity	HLA-A, HLA-B, HLA-E, HLA-F, PTPRC, FCGR2B	2.34	2.61e-10
Toll-like receptor (TLR)-signaling pathway	CD40, MYD88, TLR1, TLR10, TLR4, TLR6, TLR7, TLR8	1.57	1.08e-08
Negative regulation of NK cell mediated cytotoxicity	HLA-A, HLA-B, HLA-E, HLA-F	2.26	1.74e-06
Protection from NK cell mediated cytotoxicity	HLA-A, HLA-B, HLA-E	2.56	1.96e-05
Negative regulation of T cell mediated cytotoxicity	PTPRC, FCGR2B	2.32	0.00038
T cell activation	HLA-A, HLA-E, PTPRC, CCL19, CLEC7A	1.17	0.0013

Table 9
Biological processes linked to 74 upregulated genes associated to Dendritic cells (DCs) activity in Former Smoker LUAD patients with high levels of AIM2.

Biological Process	Genes in the network	Network strength	FDR
Regulation of immune response	TMEM173, TICAM1, MAVS, BIRC3, BIRC2, RELB, TLR4, HMGB1, IL4R, CADM1, CD40, ITGAM, CCL5, CD86, PTPRC, CD274, ADAM8, HFE, HLA-A, HLA-B, HLA-C, HLA-E, HLA-F, HLA-DQA1, HLA-DQA2, HLA-DQB1, HLA-DQB2, HLA-DMB, HLA-DRA, HLA-G, HLA-DPA1, HLA-DRB1, HLA-DPB1, HLA-DRB5	1.11	2.53e-27
Positive regulation of immune response	TMEM173, TICAM1, MAVS, RELB, TLR4, HMGB1, IL4R, CADM1, CD40, ITGAM, CCL5, CD86, PTPRC, CD274, ADAM8, HLA-A, HLA-B, HLA-E, HLA-F, HLA-DQA1, HLA-DQA2, HLA-DQB1, HLA-DQB2, HLA-DMB, HLA-DRA, HLA-G, HLA-DPA1, HLA-DRB1, HLA-DPB1, HLA-DRB5	1.23	1.11e-26
Regulation of cytokine production	TMEM173, TICAM1, MAVS, BIRC3, BIRC2, RELB, TLR4, MYD88, TLR2, CD14, LRP1, HMGB1, IL4R, CADM1, CD40, PTPRC, CD86, CD274, CD2, ADAM8, HLA-A, HLA-E, HLA-DPA1, HLA-DRB1, HLA-G, HLA-B, HLA-DPB1, HLA-F, HFE	1.13	3.88e-23
Inflammatory response	ADAM8, BCL6, CCL5, CD14, CD40, CXCL10, CXCL9, HLA-DRB1, HMGB1, IL4R, ITGAM, LRP1, LY75, MYD88, NOTCH2, RELB, TICAM1, TLR2, TLR4, TLR6, TLR8	1.03	7.05e-14
Response to cytokines	BIRC2, BIRC3, CCL5, CD14, CD274, CD40, CSF2, CXCL10, CXCL16, CXCL9, HLA-DPA1, HLA-DQB2, IL3RA, IL4R, MAVSMRC1, MYD88, NFIL3, RELB, STING1, TLR2, TLR4	0.88	1.01e-11
Toll-like receptor (TLR)-signaling pathway	CD14, CD40, MYD88, TICAM1, TLR2, TLR4, TLR6, TLR8	1.56	1.41e-08
Negative regulation of Natural Killer cell mediated cytotoxicity	HLA-A, HLA-B, HLA-E, HLA-F, HLA-G	2.03	2.73e-07
Tolerance induction	CD274, HLA-B, HLA-G, HMGB1,	1.91	2.04e-05

median survival = 45 months) than those who were inflammasome profile negative (n = 67, median survival = 23 months) (Fig. 7i, red vs black line).

Taken altogether these data support that AIM2 participates to the LUAD malignancy with an ensuing dismal prognosis and that the inflammasome profile positivity can exacerbate the role of AIM2 in Non-Smoker and Smoker, but not Former, LUAD patients, implying a dual differential activity of AIM2 in the lung.

4. Discussion

Increased activity of the inflammasomes have been related to chronic inflammation in several pathologies. In this study we found that the AIM2 inflammasome is strictly correlated to an inflammatory profile characterized by inflammasome-dependent and independent cytokines that can participate to the recruitment of resting/inactive DCs and immunosuppressive T cells that collaborate to create an immunosuppressive tumor environment facilitating tumor growth.

In previous studies, we found that the AIM2 inflammasome is involved in lung inflammation responsible for the emphysema-like, collagen deposition and chronic mucus production typical of smoker subjects. In this study, we found that although the absence of mucus-related inflammation, mice exposed to smoking and then to room-air still had emphysema-like features, correlated to lung infiltration of DCs which were not in their active form, rather, they were associated to an immunosuppressive environment. These results well mimicked what happens in humans, exploring a public transcriptomic dataset. In support, we already found that plasmacytoid DCs expressed AIM2 when recruited to the lung of NSCLC patients [15], exerting an immunosuppressive effect as observed in the melanoma microenvironment [29]. In support of this, Fukuda and collaborators [29] demonstrated that the vaccination with AIM2-deficient DCs improves the efficacy of both adoptive T cell therapy and anti–PD-1 immunotherapy for cold tumors. The deficiency of AIM2 in DCs promoted the infiltration of CD8 + T cells while limiting the accumulation of regulatory T cells through the production of CXCL10 [30]. On the other hand, AIM2 was able to control the onset of the experimental autoimmune encephalomyelitis (EAE), via the inhibition of DNA-PK-AKT3 [30], further implying its immunosuppressive role. In this study, we found that the absence of active myeloid DCs (mDCs) as well as Treg and resting NK cells in AIM2 positive LUAD patients could underly an immunosuppressive lung microenvironment, as already observed in our previous studies. However, it has to be pointed out that the role of AIM2 in infiltrated DCs was associated to the negative regulation of the cytotoxic anti-tumor immunity, but its immunosuppressive activity still needs further studies to be completely elucidated. Another strong support regarding the limitation of lung

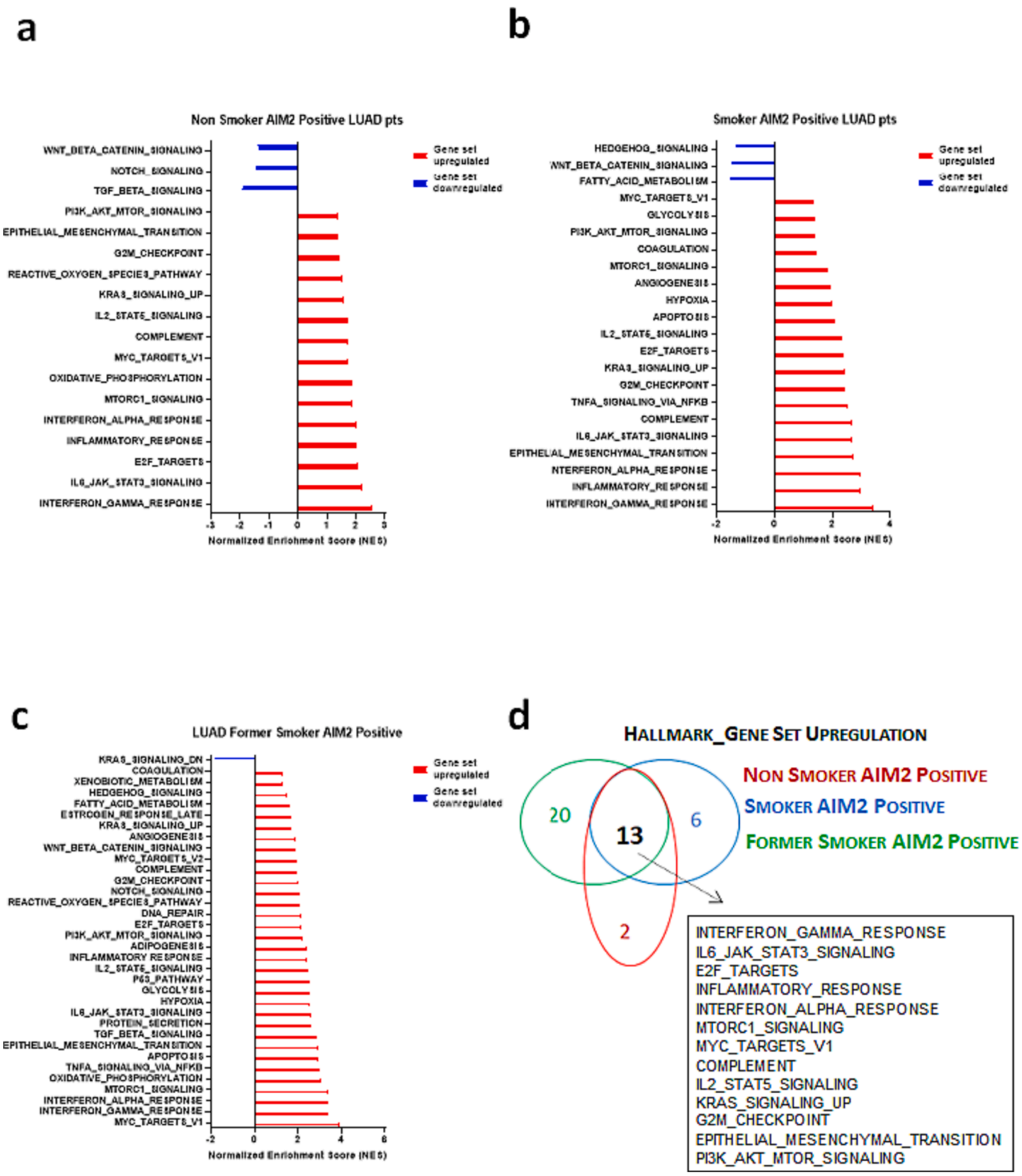

Fig. 6. Common and uncommon hallmark gene set in LUAD patients with high AIM2 mRNA levels and different smoking habits. Histogram for the normalized enrichment scores (NES) derived from Gene set enrichment analysis (GSEA) simulation in Non-Smoker (**a**), Smoker (**b**) and Former Smoker (**c**) LUAD patients with high AIM2 mRNA levels against Hallmark gene sets. **d**) Venn's diagram showing common and uncommon upregulated Hallmark gene sets in Non-Smoker (red), Smoker (light blue) and Former Smoker (green) LUAD patients with high expression of AIM2. (For interpretation of the references to colour in this figure legend, the reader is referred to the web version of this article.)

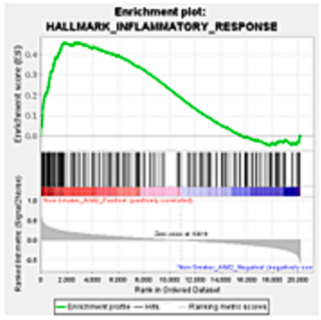

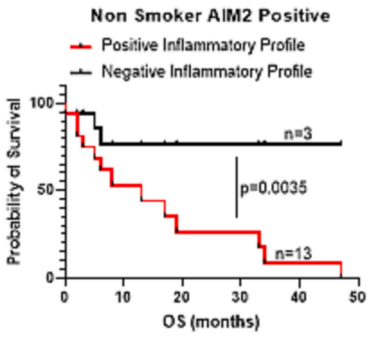

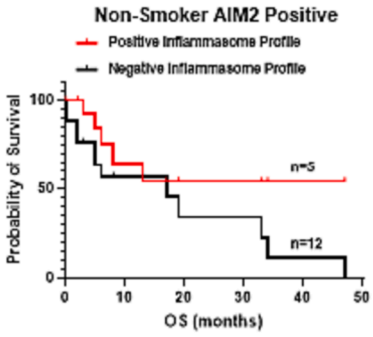

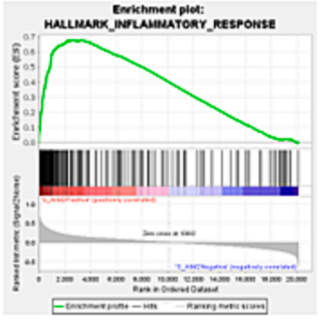

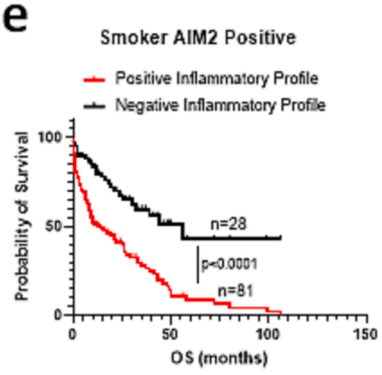

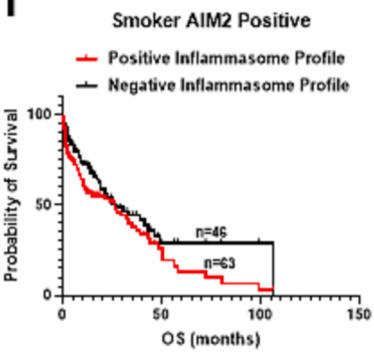

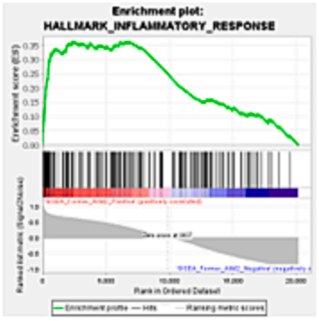

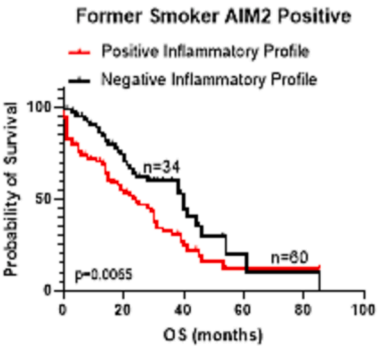

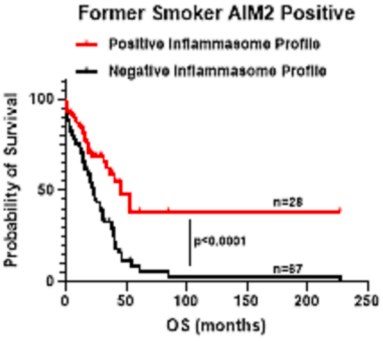

(caption on next page)

Fig. 7. Prognosis related to AIM2 positivity was both inflammasome and non-inflammasome-dependent. GSEA analysis was performed according to the hallmark database and the enrichment plot associated to the inflammatory response in Non-Smoker (**a**), Smoker (**d**) and Former Smoker (**g**) LUAD patients with high AIM2 mRNA levels. Survival curve of AIM2 Positive Non-Smoker (**b**), Smoker (**e**) and Former Smoker (**h**) LUAD patients according to positivity or negativity to the identified transcriptomic Inflammatory Profile. Profile Positive (red line) indicates patients who were positive to AIM2 and who had higher expression of at least to the 80 % of the above selected genes (according to the AUC value > 0.8) compared to the chosen cut-off; 2. Profile Negative (black line) indicates patients with high expression of AIM2 and with lower expression of the above selected genes (according to the AUC value > 0.8) compared to the chosen cut-off. Survival curve of AIM2 Positive Non-Smoker (**c**), Smoker (**f**) and Former Smoker (**i**) LUAD patients according to positivity or negativity to the identified transcriptomic Inflammasome Profile. Profile Positive (red line) indicates patients with high expression of AIM2 and with higher expression of at least 3 out of 4 genes (CASP1, IL1B, IL18, IL1A) compared to the chosen cut-off; Profile Negative (black line) indicates patients with high expression of AIM2 and with higher expression of less of 3 out of 4 genes (CASP1, IL1B, IL18, IL1A). Log-rank test was performed to statistically analyze the survival rate between the groups. (For interpretation of the references to colour in this figure legend, the reader is referred to the web version of this article.)

inflammation derives by AIM2 knockout mice exposed to smoking. The authors demonstrated that the genetic ablation of AIM2 increased neutrophil recruitment and derived airway inflammation in a COPD mouse model [7]. Here, we demonstrated that, first, AIM2 is present in the tumor tissue, and second, that its expression is correlated to the TNM stage and immunosuppressive environment. However, although the immunohistochemical analysis and the transcriptomic data, it still remains to be elucidated whether the pro-tumorigenic role of AIM2 inflammasome in LUAD is due to its expression in structural tumor cells and/or immune infiltrated cells. Canonical and non-canonical inflammasome activation has been described in both stromal and hematopoietic cells, although divergent functions of the complex are reported depending on the experimental model and on the cell type [31]. We previously demonstrated that caspase-11, which is involved in the non-canonical inflammasome pathway, has a relevant role in structural epithelial cells where it drives towards lung cancer establishment and progression in a mouse model of carcinogen-induced lung carcinogenesis [32]. However, we also found that air pollution and cigarette smoke, two common risk factors for lung cancer, can lead to the activation of the inflammasome in circulating cells [20,33,34,35]. Thus, our hypothesis is that AIM2 expression is prevalent in tumor-recruited myeloid cells, especially DCs and Treg, where this receptor can drive toward an immunosuppressive phenotype favoring tumor progression and tumor-immune escape. Therefore, further studies are needed to better investigate the expression and role of AIM2 in structural and immune cells in the tumor-microenvironment.

In conclusion, this study demonstrates that 1. AIM2 participates to lung chronic inflammation facilitating the immunosuppressive environment, and 2. that AIM2 can facilitate tumor growth via the induction of driver oncogenes, such as KRAS, MTOR, MYC, which were enriched in the three groups of LUAD patients beyond their status of smoking (Fig. 6d). Therefore, we, first of all, can confirm that besides the smoking habit, sex and age, AIM2 contributes to LUAD and then that it can sign an inflammatory profile in the lung of LUAD patients. In this regard, the poor survival associated to the expression of the AIM2 receptor was related to the inflammasome-dependent IL-1-like cytokines in Non-Smoker and Smoker LUAD patients, but not in Former Smokers (Fig. 7). Former Smoker LUAD patients with poorer prognosis were AIM2 positive but negative to the inflammasome profile. This could be related to the already described activity of AIM2 independent from the caspase-1 complex [6,20,36]. The inflammasome-independent activity of AIM2 still needs clarification and will be the object of future studies. Nevertheless, it was proved that it can have a crosstalk with cGAS (cyclic-GMP-AMP synthase)-STING (stimulator of interferon genes) signaling pathway, responsible for IFN type I and II response, that was also observed in the present data (Fig. 6) [37,38]. Recently, cGAS has been described as another cytoplasmic dsDNA sensor that catalyzes the synthesis of cyclic-guanosine monophosphate (GMP)-adenosine monophosphate (AMP)-nucleotide (cGAMP), which binds and activates the adaptor protein STING, also known as TMEM173 [39]. It was suggested that dsDNA could induce inflammasome activation through an AIM2-independent cGAS-STING pathway [40]. Our RNA-seq analysis demonstrated that AIM2 positive Former Smoker, but not Smoker, LUAD patients, were characterized by upregulation of both CGAS and TMEM173 genes, suggesting that inflammasome-independent function of AIM2 could occur in LUAD patients who stopped smoking. According to these data it is possible to speculate that self-DNA and cytoplasmic dsDNA released by cancer cells as a byproduct of genomic instability could activate both AIM2 and cGAS/STING pathways to promote tumor growth [41], most likely explaining an independent inflammasome activity of AIM2. Nevertheless, further studies are needed define a non-inflammasome activity of AIM2.

The latent IL-1-dependent lung inflammation associated to the establishment of an AIM2 positive immunosuppressive lung microenvironment renders the lung a context where harmful stimuli can establish a pro-tumor environment. In support to this concept, the analysis of RNA-seq database from LUAD patients was associated to increased recruitment of both innate immune cells, especially resting mDCs unable to present antigens and therefore leading to robust peripheral CD8 + T cell tolerance, and adaptive immunity cells, especially CD4 positive memory T cells, which role in LUAD progression is well-known [1,2,10]. Of particular interest, we found that Former Smoker LUAD patients who had higher expression of AIM2 were characterized by an increased infiltration of resting myeloid DCs (mDCs) compared to patients with lower expression of AIM2, supporting the data about the recruitment of inactive AIM2-expressing DCs into the lung of former smoking mice, as observed by Fukuda et al. [29]. Based on the inactivity of mDCs and the immunosuppressive environment, AIM2 positive LUAD patients are characterized by cancer progression and dismal prognosis. In this regard, we found that DCs and T cell population highly recruited in the tumor tissues of AIM2 positive LUAD patients were characterized by the upregulation of genes associated to both pro-inflammatory/immunostimulatory (i.e. cellular response to IL-1, cytokines mediated signaling pathway, positive regulation of IL-1β) and immunosuppressive (i.e. regulation of tolerance induction, regulation of T cell anergy, regulation of TGF-β production) pathways, conditions that favor tumor immune escape typical of lung cancer progression [15]. To note, in our previous study, we found that AIM2 was highly expressed in DCs, identified as $CD11c^{+}CD11b^{int}F4/80^{-}$ cells, recruited into the lungs of mice exposed to nose-only cigarette smoke exposure [6]. Interestingly, the analysis of DCs associated genes highlights that the cancerous tissues of AIM2 positive LUAD patients were characterized by the upregulation of genes correlated to the release of pro-inflammatory mediators (i.e. regulation of IL-1β production and cytokine-mediated signaling pathway), which play an important role in maintaining chronic inflammation, promoting the transformation of malignant epithelial cells, inhibiting tumor immune surveillance, and promoting tumor metastasis [1,2,6,10].

Despite the encouraging results, our study still has some limitations. First, since we analyzed one single dataset of patients with LUAD and different smoking status, the prognostic value of our data needs to be validated in a greater number of Non-Smoker, Smoker and Former Smoker LUAD patients. Second, the molecular mechanism by which AIM2 upregulation drives the progression of LUAD in an inflammasome-dependent and independent manner, as well as in what cell type AIM2 is relevant, still needs to be examined.

Table 10
ROC analysis of genes upregulated in the hallmark gene set 'Inflammatory response' in Non-Smoker LUAD patients with high levels of AIM2 according to the GSEA analysis. In italic the gene which AUC was ≥ 0.8.

	AUC	Cut-off	Sensitivity	Specificity
SELL	*0.8139*	*>1.568*	*80.95*	*72.73*
CXCL10	0.7706	>1.255	71.43	63.64
CXCL9	0.7619	>1.646	71.43	63.64
TNFRSF9	0.7662	>0.6553	76.19	72.73
LTA	0.7489	>0.5450	71.43	63.64
CD48	0.7706	>1.613	76.19	72.73
CXCR6	0.7403	>0.9908	71.43	63.64
SLAMF1	0.7403	>0.7681	71.43	63.64
CCL5	0.7273	>1.707	66.67	63.64
GP1BA	0.7359	>0.4611	71.43	63.64
NPFFR2	0.7749	>0.2623	76.19	72.73
EBI3	0.7619	>0.6787	76.19	63.64
CD70	0.7056	>0.4602	71.43	63.64
SLC1A2	0.6926	>0.6280	66.67	63.64
LCP2	0.7316	>1.847	71.43	63.64
HIF1A	0.7489	>3.729	76.19	72.73
IL18RAP	0.7056	>0.4317	66.67	63.64
GCH1	0.7273	>1.470	71.43	63.64
RGS16	0.6926	>1.900	66.67	45.45
TLR1	0.645	>1.397	61.9	45.45
GPR183	0.71	>1.506	71.43	63.64
BEST1	0.6494	>0.7111	61.9	45.45
CXCL11	0.6364	>0.7620	61.9	54.55
CCL7	0.71	>0.4916	71.43	72.73
IL2RB	0.7056	>1.507	71.43	63.64
FFAR2	0.6407	>0.5692	61.9	54.55
FPR1	0.6494	>1.345	61.9	54.55
IL1R1	0.6753	>3.341	66.67	63.64
NAMPT	0.632	>3.287	61.9	54.55
LPAR1	0.6277	>1.530	66.67	63.64
TACR1	0.6494	>0.5768	61.9	54.55
STAB1	0.6364	>2.093	61.9	54.55
SLC31A2	0.7143	>1.661	71.43	54.55
GPR132	0.6667	>1.289	66.67	63.64
CYBB	0.6753	>2.852	66.67	63.64
RGS1	0.619	>2.286	61.9	54.55
IL7R	0.6537	>1.207	61.9	54.55
C3AR1	0.697	>1.675	66.67	54.55
CCR7	0.6061	>1.154	57.14	54.55
PDE4B	0.632	>1.459	61.9	54.55
LYN	0.7662	>3.224	76.19	72.73
CSF1	0.6667	>1.968	66.67	63.64
CD40	0.645	>2.013	66.67	63.64
IL10	0.645	>0.5396	66.67	63.64
NLRP3	0.5931	>0.9452	57.14	54.55
PDPN	0.6364	>1.846	61.9	54.55
CXCL8	0.6147	>1.612	71.43	63.64
TPBG	0.6104	>2.045	66.67	54.55
IL15	0.645	>0.9449	61.9	54.55
CLEC5A	0.6234	>1.352	61.9	54.55
IL10RA	0.6797	>2.004	66.67	63.64
TLR2	0.5758	>2.356	47.62	45.45
CSF3R	0.5541	>0.3727	52.38	63.64
ICAM1	0.5931	>5.043	57.14	54.55
ATP2C1	0.6277	>3.215	57.14	54.55
PCDH7	0.619	>1.549	57.14	54.55
IL15RA	0.632	>1.535	61.9	54.55
NFKBIA	0.6104	>3.571	57.14	54.55
CCL20	0.5801	>1.247	57.14	54.55
CMKLR1	0.697	>1.588	66.67	63.64
IFITM1	0.5931	>3.979	57.14	54.55
DCBLD2	0.5801	>2.641	57.14	54.55
P2RX7	0.6104	>0.9509	57.14	54.55
OSMR	0.6061	>3.246	57.14	54.55
IRF1	0.5931	>2.445	57.14	45.45
SPHK1	0.5758	>1.215	57.14	54.55

5. Conclusions

Our present and previous studies [6,13] demonstrated that AIM2 inflammasome is involved in lung carcinogenesis either in a canonical and non-canonical manner. These latter studies were performed on

Table 11
ROC analysis of genes upregulated in the hallmark gene set 'Inflammatory response' in Smoker LUAD patients with high levels of AIM2 according to the GSEA analysis. In italic the gene which AUC was ≥ 0.8.

	AUC	Cut-off	Sensitivity	Specificity
CXCL9	*0,8555*	*<2,223*	*87,1*	*74,14*
TNFRSF9	*0,8578*	*<0.6379*	*80,65*	*75*
IL2RB	*0,8566*	*<1.565*	*83,87*	*75*
CXCL10	*0,8497*	*<1.524*	*80,65*	*79,31*
CCL5	*0,8096*	*<1.836*	*80,65*	*75,86*
LTA	*0,8113*	*<0.4894*	*80,65*	*73,28*
CXCR6	*0,8194*	*<1.063*	*80,65*	*75*
IRF1	*0,8227*	*<2.584*	*77,42*	*69,83*
LCK	0,7916	<1.366	74,19	67,24
SLAMF1	*0,8211*	*<0.7810*	*80,65*	*72,41*
CXCL11	*0,8052*	*<0.9204*	*80,65*	*70,69*
IL10RA	0,7963	<2.020	77,42	67,24
EBI3	*0,8202*	*<0.6694*	*70,97*	*70,69*
LCP2	*0,8052*	*<1.801*	*80,65*	*73,28*
IL15RA	*0,8233*	*<1.562*	*80,65*	*72,41*
PLAUR	0,7665	<2.941	70,97	60,34
IL18RAP	0,7627	<0.5554	77,42	63,79
IL1B	0,7805	<0.9726	77,42	77,59
CD70	0,7766	<0.4484	74,19	68,97
EMP3	0,7963	<1.846	74,19	73,28
C3AR1	0,7649	<1.738	74,19	62,93
SLC31A2	0,7882	<1.686	80,65	66,38
PTAFR	0,7665	<1.280	77,42	60,34
SELL	0,7863	<1.387	77,42	68,97
CYBB	0,7593	<2.796	70,97	68,1
TNFAIP6	0,7521	<0.9580	70,97	65,52
LYN	0,7665	<2.965	70,97	70,69
STAB1	0,7807	<2.373	74,19	67,24
P2RX7	0,7351	<0.9305	70,97	54,31
SPHK1	0,7354	<1.442	80,65	55,17
TLR1	0,7271	<1.385	70,97	59,48
ADGRE1	0,7707	<0.5709	77,42	66,38
RIPK2	0,7579	<1.878	74,19	67,24
CD48	0,7429	<1.501	70,97	63,79
SERPINE1	0,7187	<2.707	70,97	65,52
DCBLD2	0,6492	<2.615	61,29	61,21
CMKLR1	0,7482	<1.551	70,97	68,97
CSF1	0,7429	<1.884	70,97	64,66
IL7R	0,7304	<1.178	70,97	70,69
IL15	0,7779	<0.9543	80,65	68,97
ADM	0,7098	<1.500	74,19	62,07
PIK3R5	0,7424	<1.350	74,19	66,38
FPR1	0,7721	<1.324	83,87	62,07
NLRP3	0,7337	<0.9678	74,19	61,21
NOD2	0,7215	<1.078	70,97	62,07
PDPN	0,7065	<1.796	67,74	58,62
CCR7	0,746	<1.005	74,19	62,07
CD40	0,6798	<2.085	74,19	54,31
CXCL8	0,6951	<1.998	74,19	65,52

LUAD patients' samples. We demonstrated that AIM2 is involved in LUAD typical immunosuppressive environment based on the TNM stage. In this regard, AIM2 can accelerate the upregulation of tolerogenic profiles which are associated to dismal prognosis of LUAD patients.

Ethical approval

Human samples in this study were obtained by patients diagnosed of LUAD, undergoing surgical resection according to GLAD Study (number of approval from the LMU Ethical Committee #623-15), registered by the German Clinical Trials Register.

All animal experiments were performed under protocols that followed the Italian and European Community Council for Animal Care (2010/63/EU). This study was carried out in strict accordance with the recommendations in the Guide for the Care and Use of Laboratory Animals of the National Institutes of Health. The protocol was approved by the Committee on the Ethics of Animal Experiments of the University of Salerno and by National Institutes of Health with the approval number 985/2017).

Table 12
ROC analysis of genes upregulated in the hallmark gene set 'Inflammatory response' in Former Smoker LUAD patients with high levels of AIM2 according to the GSEA analysis. In italic the gene which AUC was ≥0.8.

	AUC	Cut-off	Sensitivity	Specificity
LCP2	*0,9387*	*>1.560*	*90,2*	*87,5*
SLC31A2	*0,9216*	*>1.437*	*86,27*	*80*
IL2RB	*0,9218*	*>1.385*	*85,29*	*80*
CD69	*0,9311*	*>0.9850*	*90,2*	*80*
C3AR1	*0,9233*	*>1.344*	*86,27*	*85*
RGS1	*0,9049*	*>2.130*	*83,33*	*82,5*
CD40	*0,9132*	*>1.600*	*82,35*	*80*
C5AR1	*0,8941*	*>1.296*	*88,24*	*82,5*
FPR1	*0,9061*	*>1.050*	*86,27*	*82,5*
CYBB	*0,8975*	*>2.294*	*84,31*	*82,5*
IRF1	*0,8865*	*>2.314*	*84,31*	*77,5*
CD48	*0,9103*	*>1.385*	*81,37*	*80*
LTA	*0,8993*	*>0.4637*	*83,33*	*82,5*
TNFRSF9	*0,9186*	*>0.5124*	*86,27*	*85*
AHR	*0,873*	*>3.289*	*81,37*	*77,5*
EMP3	*0,902*	*>1.728*	*89,22*	*82,5*
HIF1A	*0,8571*	*>3.481*	*78,43*	*75*
IL7R	*0,8841*	*>1.132*	*80,39*	*77,5*
TNFRSF1B	*0,8417*	*>2.223*	*77,45*	*72,5*
CSF1	*0,8762*	*>1.682*	*82,35*	*80*
AQP9	*0,8765*	*>0.9578*	*83,33*	*77,5*
LYN	*0,9005*	*>2.762*	*85,29*	*80*
TNFAIP6	*0,8743*	*>0.7413*	*75,49*	*72,5*
SPHK1	*0,8556*	*>0.9724*	*84,31*	*72,5*
TIMP1	*0,8029*	*>4.740*	*73,53*	*72,5*
OLR1	*0,8716*	*>1.480*	*78,43*	*77,5*
OSM	*0,8745*	*>0.7350*	*82,35*	*80*
KLF6	*0,8331*	*>3.169*	*76,47*	*75*
IL4R	*0,8355*	*>2.692*	*77,45*	*72,5*
CXCL11	*0,8735*	*>0.7105*	*80,39*	*75*
PLAUR	*0,8809*	*>2.092*	*87,25*	*82,5*
ICAM1	*0,8623*	*>3.673*	*83,33*	*75*
ICOSLG	*0,8468*	*>1.187*	*84,31*	*77,5*
TAPBP	*0,8005*	*>4.353*	*75,49*	*70*
CXCL10	*0,85*	*>1.350*	*77,45*	*75*
PTPRE	*0,8103*	*>2.206*	*77,45*	*75*
SLC31A1	*0,8591*	*>2.508*	*83,33*	*77,5*
RTP4	*0,835*	*>0.8671*	*82,35*	*77,5*
OSMR	*0,8473*	*>2.884*	*77,45*	*75*
NAMPT	*0,8208*	*>3.326*	*71,57*	*70*
AXL	*0,8571*	*>2.068*	*79,41*	*77,5*
HRH1	*0,8181*	*>1.303*	*72,55*	*70*
PSEN1	0,7824	>2.989	72,55	70
MMP14	*0,8375*	*>3.653*	*74,51*	*72,5*
RELA	0,7728	>2.978	78,43	67,5
MEFV	*0,8333*	*>0.4419*	*81,37*	*67,5*
TLR2	*0,8765*	*>1.856*	*83,33*	*80*
IFITM1	*0,852*	*>2.859*	*84,31*	*77,5*
BST2	*0,8225*	*>2.812*	*76,47*	*75*
LY6E	*0,8083*	*>3.708*	*80,39*	*67,5*
NFKBIA	0,7801	>3.479	73,53	67,5
ADRM1	0,7525	>2.794	71,57	67,5
EDN1	0,7961	>1.457	68,63	65
GNA15	0,789	>1.695	78,43	67,5
ABCA1	0,5708	<0.8203	52,94	52,5
IFNGR2	*0,839*	*>3.015*	*77,45*	*72,5*
ATP2A2	0,7326	>4.844	65,69	65
ITGB8	*0,8426*	*>1.059*	*80,39*	*75*
RIPK2	*0,8216*	*>1.745*	*75,49*	*72,5*
LDLR	0,738	>2.529	71,57	67,5
GNAI3	0,7973	>2.883	74,51	72,5

Funding

This study was supported by grant FESR-POR-MOVIE in favor of AP and RS, by FARB2021 in favor of MT, by FARB2022 in favor of RS. PMH is funded by a Fellowship and grants from the National Health and Medical Research Council (NHMRC) of Australia (1175134) and by UTS. This article is based upon work from COST Action IMMUNO-model CA21135, supported by COST (European Cooperation in Science and Technology) https://www.immuno-model.eu/.

CRediT authorship contribution statement

Chiara Colarusso: Data curation, Formal analysis, Methodology, Writing – original draft. **Michela Terlizzi:** Data curation, Formal analysis, Methodology. **Anna Falanga:** Software, Validation. **Georgious Stathopoulos:** Resources. **Luigi De Lucia:** Methodology. **Phillip M. Hansbro:** Visualization, Writing – review & editing. **Aldo Pinto:** Funding acquisition, Visualization, Writing – review & editing. **Rosalinda Sorrentino:** Funding acquisition, Conceptualization, Investigation, Visualization, Supervision, Data curation, Formal analysis, Methodology, Project administration.

Declaration of Competing Interest

The authors declare that they have no known competing financial interests or personal relationships that could have appeared to influence the work reported in this paper.

Data availability

The datasets used and/or analyzed during the current study are available from the corresponding author on reasonable request.

Acknowledgements

We thank Dr. Piera Maiolino for her help with clinical data management.

Appendix A. Supplementary material

Supplementary data to this article can be found online at https://doi.org/10.1016/j.intimp.2023.110990.

References

[1] G. Caramori, P. Ruggeri, S. Mumby, A. Ieni, F. Lo Bello, V. Chaminka, C. Donovan, F. Andò, F. Nucera, I. Coppolino, G. Tuccari, P.M. Hansbro, I.M. Adcock, Molecular links between COPD and lung cancer: new targets for drug discovery? Expert opinion in therapeutic, Targets 23 (2019) 539–553, https://doi.org/10.1080/14728222.2019.1615884.

[2] H. Sung, J. Ferlay, R.L. Siegel, M. Laversanne, I. Soerjomataram, A. Jemal, F. Bray, Global cancer statistics 2020: GLOBOCAN estimates of incidence and mortality worldwide for 36 cancers in 185 countries, CA Cancer J. Clin. 71 (2021) (2020) 209–249, https://doi.org/10.3322/caac.21660.

[3] F. Nucera, F. Lo Bello, S.S. Shen, P. Ruggeri, I. Coppolino, A. Di Stefano, C. Stellato, V. Casolaro, P.M. Hansbro, I.M. Adcock, G. Caramori, Role of atypical chemokines and chemokine receptors pathways in the pathogenesis of COPD, Curr. Med. Chem. 28 (2021) 2577–2653, https://doi.org/10.2174/0929867327999200819145327.

[4] Centers for Disease Control and Prevention. <https://www.cdc.gov/cancer/lung/basic_info/risk_factors.htm>.

[5] C. Faselis, J.A. Nations, C.J. Morgan, J. Antevil, J.M. Roseman, S. Zhang, G. C. Fonarow, H.M. Sheriff, G.D. Trachiotis, R.M. Allman, P. Deedwania, Q. Zeng-Trietler, D.D. Taub, A.A. Ahmed, G. Howard, A. Ahmed, Assessment of lung cancer risk among smokers for whom annual screening is not recommended, JAMA Oncol. 8 (2022) 1428–1437, https://doi.org/10.1001/jamaoncol.2022.2952.

[6] C. Colarusso, M. Terlizzi, A. Lamort, I. Cerqua, F. Roviezzo, G. Stathopoulos, A. Pinto, R. Sorrentino, Caspase-11 and AIM2 inflammasome are involved in smoking-induced COPD and lung adenocarcinoma, Oncotarget 12 (2021) 1057–1071, https://doi.org/10.18632/oncotarget.27964.

[7] C. Donovan, R.Y. Kim, I. Galvao, A.G. Jarnicki, A.C. Brown, B. Jones-Freeman, H. M. Gomez, R. Wadhwa, E. Hortle, R. Jayaraman, H. Khan, S. Pickles, P. Sahu, V. Chimankar, X. Tu, M.K. Ali, J.R. Mayall, D.H. Nguyen, K.F. Budden, V. Kumar, K. Schroeder, A.A. Robertson, M.A. Cooper, P.A. Wark, B.G. Oliver, J.C. Horvat, P. M. Hansbro, Aim2 suppresses cigarette smoke-induced neutrophil recruitment, neutrophil caspase-1 activation and anti-Ly6G-mediated neutrophil depletion, Immunol. Cell Biol. 100 (2022) 235–249, https://doi.org/10.1111/imcb.12537.

[8] J.W. Pinkerton, R.Y. Kim, A.A. Robertson, J.A. Hirota, L.G. Wood, D.A. Knight, M. A. Cooper, L.A.J. O'Neill, J.C. Horvat, P.M. Hansbro, Inflammasomes in the lung, Mol. Immunol. 8 (2017) 1615, https://doi.org/10.1016/j.molimm.2017.01.014.

[9] M. Moossavi, N. Parsamanesh, A. Bahrami, S.L. Atkin, A. Sahebkar, Role of the NLRP3 inflammasome in cancer, Mol. Cancer 17 (2018) 158, https://doi.org/10.1186/s12943-018-0900-3.

[10] M. Terlizzi, V. Casolaro, A. Pinto, R. Sorrentino, Inflammasome: cancer's friend or foe? Pharmacol. Ther. 143 (2014) 24–33, https://doi.org/10.1016/j.pharmthera.2014.02.002.

[11] K. Schroder, J. Tschopp, The inflammasomes, Cell 140 (2010) 821–832, https://doi.org/10.1016/j.cell.2010.01.040.
[12] E.K. Robinson, P. Jagannatha, S. Covarrubias, M. Cattle, V. Smaliy, R. Safavi, B. Shapleigh, R. Abu-Shumays, M. Jain, S.M. Cloonan, M. Akeson, A.N. Brooks, S. Carpenter, Inflammation drives alternative first exon usage to regulate immune genes including a novel iron-regulated isoform of Aim2, Elife 10 (2021) e69431.
[13] M. Terlizzi, V.G. Di Crescenzo, G. Perillo, A. Galderisi, A. Pinto, R. Sorrentino, Pharmacological inhibition of caspase-8 limits lung tumour outgrowth, Br. J. Pharmacol. 172 (2015) 3917–3928, https://doi.org/10.1111/bph.13176.
[14] M. Terlizzi, C. Colarusso, A. Popolo, A. Pinto, R. Sorrentino, IL-1α and IL-1β-producing macrophages populate lung tumor lesions in mice, Oncotarget 7 (2016), 58181-5819210.18632/oncotarget.11276.
[15] R. Sorrentino, M. Terlizzi, V.G. Di Crescenzo, A. Popolo, M. Pecoraro, G. Perillo, A. Galderisi, A. Pinto, Human lung cancer-derived immunosuppressive plasmacytoid dendritic cells release IL-1α in an AIM2 inflammasome-dependent manner, Am. J. Pathol. 185 (2015) 3115–3124, https://doi.org/10.1016/j.ajpath.2015.07.009.
[16] H. Kong, Y. Wang, X. Zeng, Z. Wang, H. Wang, W. Xie, Differential expression of inflammasome in lung cancer cell lines and tissues, Tumour Biol. 36 (2015) 7501–7513, https://doi.org/10.1007/s13277-015-3473-4.
[17] M. Qi, D. Dai, J. Liu, Z. Li, P. Liang, Y. Wang, L. Cheng, Y. Zhan, Z. An, Y. Song, Y. Yang, X. Yan, H. Xiao, H. Shao, AIM2 promotes the development of non-small cell lung cancer by modulating mitochondrial dynamics, Oncogene 3 (2020) 1017–1031, https://doi.org/10.1038/s41388-020-1176-9.
[18] M. Terlizzi, A. Molino, C. Colarusso, C. Donovan, P. Imitazione, P. Somma, R. P. Aquino, P.M. Hansbro, A. Pinto, R. Sorrentino, Activation of the absent in melanoma 2 inflammasome in peripheral blood mononuclear cells from idiopathic pulmonary fibrosis patients leads to the release of pro-fibrotic mediators, Front. Immunol. 9 (2018), https://doi.org/10.3389/fimmu.2018.00670.
[19] C. Colarusso, M. Terlizzi, A. Molino, A. Pinto, R. Sorrentino, Role of the inflammasome in chronic obstructive pulmonary disease (COPD), Oncotarget 8 (2017) 81813–81824, https://doi.org/10.18632/oncotarget.17850.
[20] C. Colarusso, M. Terlizzi, A. Molino, P. Imitazione, P. Somma, R. Rega, A. Saccomanno, R.P. Aquino, A. Pinto, R. Sorrentino, AIM2 inflammasome activation leads to IL-1α and TGF-β release from exacerbated chronic obstructive pulmonary disease-derived peripheral blood mononuclear cells, Front. Pharmacol. 10 (2019) 257, https://doi.org/10.3389/fphar.2019.00257.
[21] A. Molino, M. Terlizzi, C. Colarusso, A. Rossi, P. Somm, A. Saglia, A. Pinto, R. Sorrentino, AIM2/IL-1α/TGF-β axis in PBMCs from exacerbated Chronic Obstructive Pulmonary Disease (COPD) patients is not related to COX-2-dependent inflammatory pathway, Front. Physiol. 10 (2019) 1235, https://doi.org/10.3389/fphys.2019.01235.
[22] L.V. Klotz, Y. Courty, M. Lindner, A. Petit-Courty, M.E. Eichhorn, I. Lilis, A. Morresi-Hauf, K.A.M. Arendt, M. Pepe, S. Giopanou, G. Ntaliarda, S.J. Behrend, M. Oplopoiou, V. Gissot, S. Guyetant, S. Marchand-Adam, J. Behr, J.C. Kaiser, R. A. Hatz, A.S. Lamort, G.T. Stathopoulos, Comprehensive clinical profiling of the Gauting locoregional lung adenocarcinoma donors, Cancer Med. 8 (2019) 1486–1499, https://doi.org/10.1002/cam4.2031.
[23] P.M. Hansbro, M.J. Hamilton, M. Fricker, S.L. Gellatly, A.G. Jarnicki, D. Zheng, S. M. Frei, G.W. Wong, S. Hamadi, S. Zhou, P.S. Foster, S.A. Krilis, R.L. Stevens, Importance of mast cell Prss31/transmembrane tryptase/tryptase-γ in lung function and experimental chronic obstructive pulmonary disease and colitis, J. Biol. Chem. 289 (2014) 18214–18227, https://doi.org/10.1074/jbc.M114.548594.
[24] T.J. Haw, M.R. Starkey, P.M. Nair, S. Pavlidis, G. Liu, D.H. Nguyen, A.C. Hsu, I. Hanish, R.Y. Kim, A.M. Collison, M.D. Inman, P.A. Wark, P.S. Foster, D.A. Knight, J. Mattes, H. Yagita, I.M. Adcock, J.C. Horvat, P.M. Hansbro, A pathogenic role for tumor necrosis factor-related apoptosis-inducing ligand in chronic obstructive pulmonary disease, Mucosal. Immunol. 9 (2016) 859–872, https://doi.org/10.1038/mi.2015.111.
[25] R. Sorrentino, A. Bertolino, M. Terlizzi, V.M. Iacono, P. Maiolino, G. Cirino, F. Roviezzo, A. Pinto, B cell depletion increases sphingosine-1-phosphate-dependent airway inflammation in mice, Am. J. Respir. Cell Mol. Biol. 52 (2015) 571–583, https://doi.org/10.1165/rcmb.2014-0207OC.
[26] M.R. Starkey, M.W. Plank, P. Casolari, A. Papi, S. Pavlidis, Y. Guo, G.J.M. Cameron, T.J. Haw, A. Tam, M. Obiedat, C. Donovan, N.G. Hansbro, D.H. Nguyen, P.M. Nair, R.Y. Kim, J.C. Horvat, G.E. Kaiko, S.K. Durum, P.A. Wark, D.D. Sin, G. Caramori, I. M. Adcock, P.S. Foster, P.M. Hansbro, IL-22 and its receptors are increased in human and experimental COPD and contribute to pathogenesis, Eur. Respir. J. 54 (2019) 1800174, https://doi.org/10.1183/13993003.00174-2018.
[27] R.Y. Kim, K.P. Sunkara, K.R. Bracke, A.G. Jarnicki, C. Donovan, A.C. Hsu, A. Ieni, E.L. Beckett, I. Galvao, S. Wijnant, F.L. Ricciardolo, A. Di Stefano, T.J. Haw, G. Liu, A.L. Ferguson, U. Palendira, P.A. Wark, G. Conickx, P. Mestdagh, G.G. Brusselle, G. Caramori, P.S. Foster, J.C. Horvat, P.M. Hansbro. A microRNA-21-mediated SATB1/S100A9/NF-κB axis promotes chronic obstructive pulmonary disease pathogenesis, Sci. Transl. Med. 13 (2021) eaav7223. 10.1126/scitranslmed.aav7223.
[28] A.M. Newman, C.L. Liu, M.R. Green, A.J. Gentles, W. Feng, Y. Xu, C.D. Hoang, M. Diehn, A.A. Alizadeh, Robust enumeration of cell subsets from tissue expression profiles, Nat. Methods 12 (2015) 453–457, https://doi.org/10.1038/nmeth.3337.
[29] K. Fukuda, K. Okamura, R.L. Riding, X. Fan, K. Afshari, N.S. Haddadi, S. M. McCauley, M.H. Guney, J. Luban, T. Funakoshi, T. Yaguchi, Y. Kawakami, A. Khvorova, K.A. Fitzgerald, J.E. Harris, AIM2 regulates anti-tumor immunity and is a viable therapeutic target for melanoma, JEM. 218 (2021) e20200962.
[30] C. Ma, S. Li, Y. Hu, Y. Ma, Y. Wu, C. Wu, X. Liu, B.G. Hu, J. Zhou, S. Yang, AIM2 microglial inflammation to prevent experimental autoimmune encephalomyelitis, J. Exp. Med. 218 (2021) e20201796.
[31] R. Karki, S.M. Man, T.N. Kanneganti. Inflammasomes and cancer. Cancer Immunol. Res. 5 (2017) 94–99. doi. 10.1158/2326-6066.CIR-16-0269.
[32] M. Terlizzi, C. Colarusso, I. De Rosa, P. Somma, C. Curcio, R.P. Aquino, L. Panico, R. Salvi, F. Zito Marino, G. Botti, A. Pinto, R. Sorrentino, Identification of a novel subpopulation of Caspase-4 positive non-small cell lung Cancer patients, J. Exp. Clin. Cancer Res. 39 (2019) 242, https://doi.org/10.1186/s13046-020-01754-0.
[33] G. De Falco, M. Terlizzi, M. Sirignano, M. Commodo, A. D'Anna, R.P. Aquino, A. Pinto, R. Sorrentino, Human peripheral blood mononuclear cells (PBMCs) from smokers release higher levels of IL-1-like cytokines after exposure to combustion-generated ultrafine particles, Sci. Rep. 7 (2017) 43016, https://doi.org/10.1038/srep43016.
[34] G. De Falco, C. Colarusso, M. Terlizzi, A. Popolo, M. Pecoraro, M. Commodo, P. Minutolo, M. Sirignano, A. D'Anna, R.P. Aquino, A. Pinto, A. Molino, R. Sorrentino, Chronic obstructive pulmonary disease-derived circulating cells release IL-18 and IL-33 under ultrafine particulate matter exposure in a caspase-1/8-independent manner, Front. Immunol. 8 (2017) 1415, https://doi.org/10.3389/fimmu.2017.01415.
[35] C. Colarusso, G. De Falco, M. Terlizzi, F. Roviezzo, I. Cerqua, M. Sirignano, G. Cirino, R.P. Aquino, A. Pinto, A. D'Anna, R. Sorrentino, The inhibition of caspase-1- does not revert Particulate Matter (PM)-induced lung immunesuppression in mice, Front. Immunol. 10 (2019) 1329, https://doi.org/10.3389/fimmu.2019.01329.
[36] C. Colarusso, M. Terlizzi, A. Maglio, A. Molino, C. Candia, C. Vitale, P.M. Hansbro, A. Vatrella, A. Pinto, R. Sorrentino, Activation of the AIM2 receptor in circulating cells of post-Covid-19 patients with signs of lung fibrosis is associated with the release of IL-1α, IFN-α and TGF-B, Front Immunol. 13 (2022), 934264 https://doi.org/10.3389/fimmu.2022.934264.
[37] D. Choubey, Type I interferon (IFN)-inducible Absent in Melanoma 2 proteins in neuroinflammation: implications for Alzheimer's disease, J. Neuroinflam. 16 (2019) 236, https://doi.org/10.1186/s12974-019-1639-5.
[38] J.W. Jones, N. Kayagaki, P. Broz, T. Henry, K. Newton, K. O'Rourke, S. Chan, J. Dong, Y. Qu, M. Roose-Girma, V.M. Dixit, D.M. Monack, Absent in melanoma 2 is required for innate immune recognition of Francisella tularensis, Proc. Natl. Sci. U.S.A. 107 (2010) 9771–9776, https://doi.org/10.1073/pnas.1003738107.
[39] K.P. Hopfner, V. Hornung, Molecular mechanisms and cellular functions of cGAS-STING signalling, Nat. Rev. Mol. Cell Biol. 21 (2020) 501–521, https://doi.org/10.1038/s41580-020-0244-x).
[40] L. Sun, J. Wu, F. Du, X. Chen, Z.J. Chen, Cyclic GMP-AMP synthase is a cytosolic DNA sensor that activates the type I interferon pathway, Science 339 (2013) 786–791, https://doi.org/10.1126/science.1232458).
[41] K.J. Mackenzie, P. Carrol, C.A. Martin, O. Murina, A. Fluteau, D.J. Simpson, N. Olova, H. Sutcliffe, J.K. Rainger, A. Leitch, cGAS surveillance of micronuclei links genome instability to innate immunity, Nature 5487668 (2017) 461–465, https://doi.org/10.1038/nature23449.